nature cell biology

C/EBPα and β couple interfollicular keratinocyte proliferation arrest to commitment and terminal differentiation

Rodolphe G. Lopez[1], Susana Garcia-Silva[1], Susan J. Moore[1], Oksana Bereshchenko[1], Ana B. Martinez-Cruz[2], Olga Ermakova[1], Elke Kurz[1], Jesus M. Paramio[2] and Claus Nerlov[1,3,4]

The transcriptional regulators that couple interfollicular basal keratinocyte proliferation arrest to commitment and differentiation are yet to be identified. Here we report that the basic region leucine zipper transcription factors C/EBPα and C/EBPβ are co-expressed in basal keratinocytes, and are coordinately upregulated as keratinocytes exit the basal layer and undergo terminal differentiation. Mice lacking both C/EBPα and β in the epidermis showed increased proliferation of basal keratinocytes and impaired commitment to differentiation. This led to ectopic expression of keratin 14 (K14) and ΔNp63 in suprabasal cells, decreased expression of spinous and granular layer proteins, parakeratosis and defective epidermal water barrier function. Knock-in mutagenesis revealed that C/EBP-E2F interaction was required for control of interfollicular epidermis (IFE) keratinocyte proliferation, but not for induction of spinous and granular layer markers, whereas C/EBP DNA binding was required for ΔNp63 downregulation and K1/K10 induction. Finally, loss of C/EBPα/β induced stem cell gene expression signatures in the epidermis. C/EBPs, therefore, couple basal keratinocyte cell cycle exit to commitment to differentiation through E2F repression and DNA binding, respectively, and may act to restrict the epidermal stem cell compartment.

The epidermis is maintained by proliferation of basal keratinocytes and their subsequent coordinated cell cycle exit, migration into the suprabasal layers, and terminal differentiation. IFE keratinocytes are shed from the skin surface and are replaced from an epidermal stem cell or progenitor pool in the K14 and K5-expressing basal layer[1,2]. Onset of differentiation is accompanied by downregulation of K14 and K5 and upregulation of K1 and K10 (ref. 3). Spinous layer cells migrate upwards, forming the stratum granulosum layer. This process involves expression of structural proteins and enzymes that generate a highly crosslinked matrix, lipids that interact with this matrix to provide impermeability to water, and keratinocyte enucleation. This upper layer of enucleated keratinocytes forms the stratum corneum[4].

Transcriptional coupling of keratinocyte proliferation, commitment and differentiation is still not understood. Loss of pRb and p107, which mediate E2F repression, simultaneously increases keratinocyte proliferation and disrupts differentiation[5]. A crucial E2F target gene could be *Myc*, which is essential for normal proliferation of IFE keratinocytes[6] and when overexpressed induces phenotypes similar to those seen when *E2f1* is overexpressed in the epidermis[7]. Another crucial regulator of epidermal keratinocytes is p63, which is required for the specification and/or maintenance of stratified epithelia during normal development[8–13]. p63 is downregulated on exit from the basal layer, a process dependent on Notch1 (ref. 14), but is independent of canonical Notch signaling[15]. The transcriptional regulators of p63 during spinous layer commitment, however, remain to be identified, as does the mechanism by which activity of the S-phase-promoting E2F/Myc complex is restricted to basal keratinocytes.

The C/EBPα and β transcription factors are expressed in the differentiating layers of the epidermis[16–18], and couple cell cycle exit with terminal differentiation in several cell types[19]. However, mice lacking C/EBPβ show only a mild perturbation of IFE keratinocyte differentiation[20], and no epidermal developmental phenotype has been reported in C/EBPα knockout mice[21]. Given their overlapping expression pattern, we examined whether C/EBPα and β promote differentiation of IFE keratinocytes in a redundant manner.

We found that epidermal ablation of both of the major C/EBP isoforms led to increased basal keratinocyte proliferation, severe defects in keratinocyte commitment and differentiation, and loss of epithelial barrier function. Knock-in mutagenesis showed that E2F repression contributes significantly to the control of C/EBP-mediated proliferation. Loss of C/EBPα and β also led to upregulation of stem-cell-specific gene expression signatures in the epidermis, ectopic Sox9 expression in IFE keratinocytes, cytoplamic translocation of NFATc1, and loss of

[1]EMBL Mouse Biology Unit, Monterotondo, 00016 Italy. [2]Molecular Oncology Unit, CIEMAT, Madrid, 28040 Spain. [3]Institute for Stem Cell Research and MRC Centre for Regenerative Medicine, University of Edinburgh, UK.
[4]Corresponding should be addressed to C.N. (e-mail: cnerlov@staffmail.ed.ac.uk)

Received 27 March 2009; accepted 10 June 2009; published online 13 September 2009; DOI: 10.1038/ncb1960

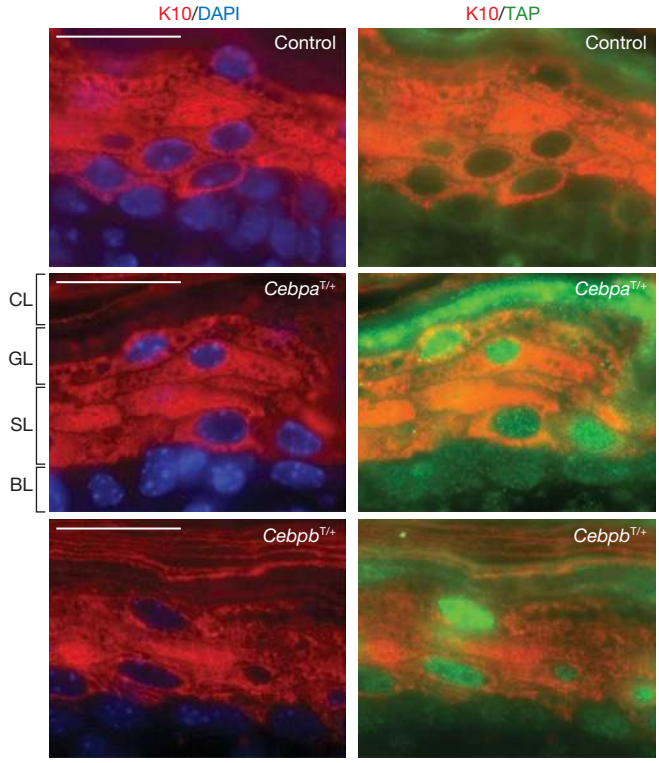

Figure 1 C/EBPα–TAP and C/EBPβ–TAP knock-in reveals the expression pattern of C/EBPα and C/EBPβ transcription factors in newborn epidermis. Immunofluorescence microscopy was performed on skin sections of newborn wild-type (Control), C/EBPα–TAP (*Cebpa*$^{T/+}$) or C/EBPβ–TAP (*Cebpb*$^{T/+}$) heterozygous knock-in mice. Sections were stained for TAP (green), K10 (red) and DAPI (blue). Scale bars, 20 μm. Abbreviations: BL, basal layer; SL, spinous layer; GL, granular layer; CL, cornified layer.

quiescence in presumptive bulge stem cells. These results identified C/EBPα and β as key transcription factors that couple loss of stem cell identity and commitment to terminal differentiation with cell cycle arrest, and subsequently execute a transcriptional program essential for epidermal barrier function.

RESULTS

Expression of C/EBPα and β in the epidermis

Different expression patterns and subcellular localization of C/EBPα and β in the epidermis have been reported in the literature, possibly because of antibody cross-reactivity with other proteins[16–18,21]. We used mouse strains carrying TAP-tagged knock-in alleles of *Cebpa*, which encodes C/EBPα, and *Cebpb*, which encodes C/EBPβ (Supplementary Information, Fig. S1). The TAP tag contains a *Staphylococcus aureus* protein A moiety that can be revealed with non-immune rabbit serum (NIRS) immunoglobulins. NIRS did not show nuclear background in the epidermis (Fig. 1), allowing the detection of low nuclear expression levels. By co-staining *Cebpa*$^{T/+}$, *Cebpb*$^{T/+}$ and control (+/+) epidermis with NIRS and monoclonal anti-K10 or K14 antibody, we observed that both C/EBPα–TAP and C/EBPβ–TAP were similarly expressed in basal keratinocyte nuclei, and that their expression was coordinately upregulated during differentiation, the highest C/EBP levels being present in the stratum granulosum (Fig. 1; Supplementary Information, Fig. S1). Their highly similar patterns of expression were thus consistent with redundant roles of C/EBPα and β in the IFE.

Defective differentiation in mice lacking C/EBPα and β in the epidermis

To genetically address the possibility of redundancy between C/EBPα and β during keratinocyte differentiation, we conditionally deleted both genes in the epidermis using floxed alleles of *Cebpb* (Supplementary Information, Fig. S2a, b), *Cebpa*[22] and the K14-Cre transgene[23]. Mice containing the resulting epidermal double knockout of both C/EBPs (EDKO mice) died 5–8 h after birth. Their skin was taut and shiny, and eyelids open (Fig. 2a; Supplementary Information, Fig. S2c). PCR analysis of EDKO epidermis showed highly efficient deletion of both genes (Fig. 2b). Loss of all *Cebpa* and *Cebpb* alleles was required for the phenotype to be seen, as animals retaining a single wild-type allele of either gene developed normally (Fig. 2c). Newborn EDKO mice showed rapid and progressive weight loss, indicating severe transepithelial water loss (Fig. 2d), but did not show a lipophilic barrier dysfunction (Fig. 2e and data not shown). Microarray analysis identified genes encoding components of the cornified envelope (*Lor*, encoding loricrin), *Flg* (encoding filaggrin), which is required for proper profilaggrin processing (*Casp14*, encoding caspase 14) and is involved in lipid processing (*Sts*, encoding steroid sulfatase) and crosslinking of cornified envelope proteins (*Tgm3*, encoding transglutaminase 3). The analysis also found that putative mediators of keratinocyte enucleation (*Casp1*, encoding caspase 1) are downregulated in EDKO mice. As expected, *Cebpa* and *Cebpb* were downregulated to an undetectable level (Supplementary Information, Table S1). Downregulation of *Cebpa*, *Cebpb*, *Sts*, *Tgm3*, *Casp1* and *Casp14* was confirmed by quantitative real-time reverse transcriptase PCR (Q-PCR; Fig. 2f, g). Histological examination revealed an immature phenotype of the IFE in EDKO mice, with fewer and smaller keratohyalin granules in the stratum granulosum and an immature non-scaling appearance of the stratum corneum (Fig. 2h) and parakeratosis. Differentiation marker analysis showed that in EDKO mice, the expression of the basal keratinocyte marker K14/K5 was expanded to suprabasal cells, and onset of K1/K10 expression (markers of suprabasal spinous layer keratinocytes) was delayed and diminished (Figs 3a, b and Supplementary Information, Fig. S3b). Expression of the terminal differentiation markers involucrin and loricrin was reduced or absent (Figs 3c, d; Supplementary Information, Fig. S3a).

Basal keratinocyte hyperproliferation in the absence of C/EBPα and β

C/EBPs are known to regulate cell proliferation[19]. Expression of keratin 6 is considered a reliable marker of IFE keratinocyte hyperproliferation. In EDKO epidermis, high levels of K6 were observed (Fig. 4a) and proliferating cell nuclear antigen (PCNA), which is normally restricted to a subset of basal keratinocytes, was uniform in the basal layer of EDKO epidermis, and expanded to the suprabasal layers where K14 is ectopically expressed (Fig. 4b). BrdU incorporation at embryonic day (E) 18.5 showed that the labelling index in EDKO epidermis was increased threefold, compared with control littermates (Fig. 4c; Supplementary Information, Fig. S3d). C/EBPα and β were thus instrumental for both basal keratinocyte cell cycle exit and their commitment to a suprabasal fate. Consistent with this result, genes known to control proliferation of basal keratinocytes *in vivo*, including *Trp63* (encoding p63), *Tgfa* (encoding TGFα), *Myc* (encoding c-Myc) and *Mycl1* (encoding L-Myc), were upregulated at the mRNA level by Q-PCR (Fig. 4d). In IFE, p63 expression is normally restricted to the basal layer and the

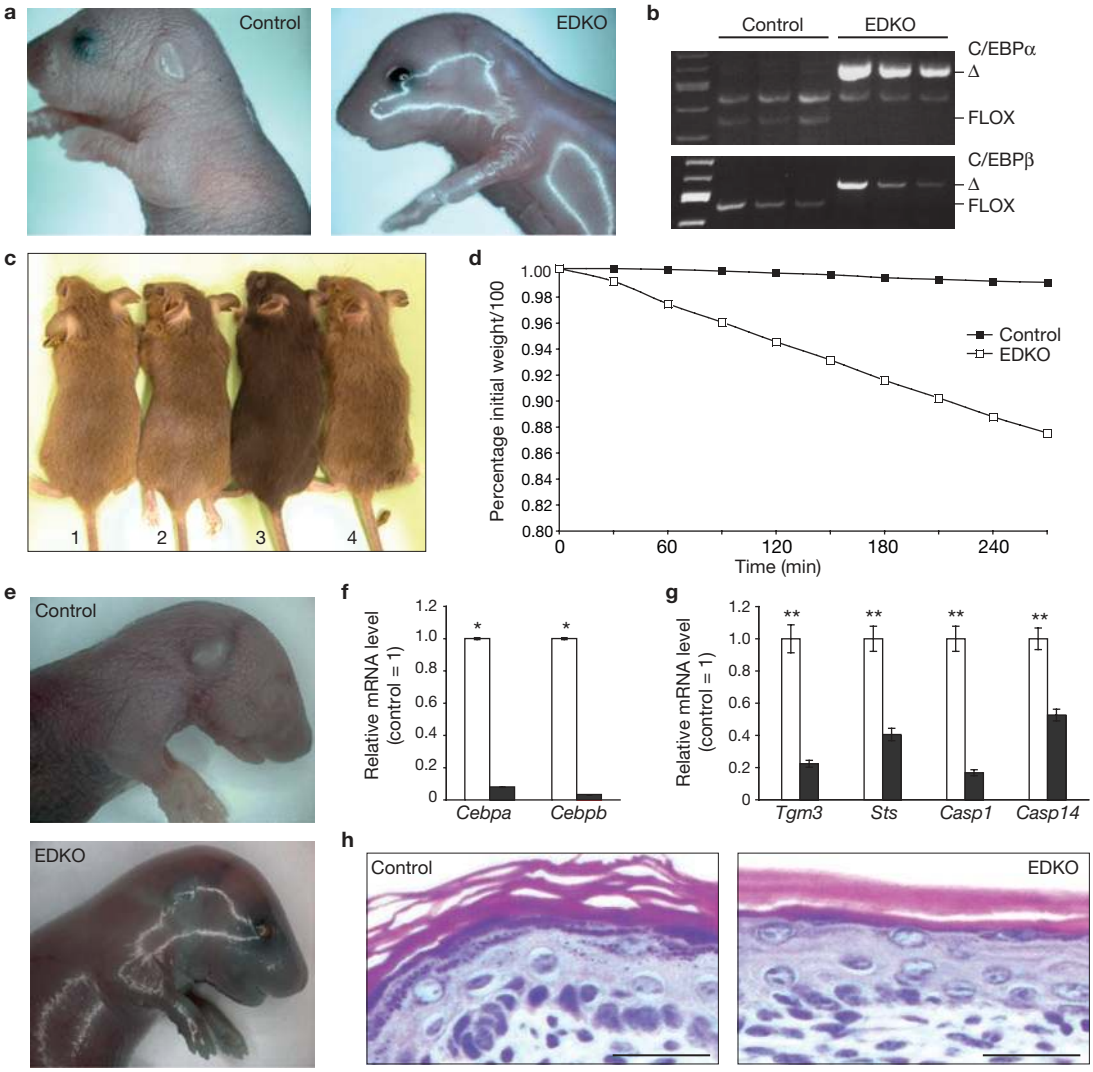

Figure 2 C/EBPα;C/EBPβ epidermis conditional knockout mice show in-to-out skin barrier dysfunction and die perinatally. (**a**) Images showing the general appearance of newborn control and EDKO pups. (**b**) PCR on genomic DNA from epidermis of *Cebpa*$^{fl/fl}$;*Cebpb*$^{fl/fl}$ (Control) and *Cebpa*$^{fl/fl}$;*Cebpb*$^{fl/fl}$;K14-Cre$^{tg/+}$ (EDKO) mice showing the recombination of Floxed alleles of C/EBPα (upper panel) or C/EBPβ (lower panel) in the presence of the K14-Cre transgene. Bands indicated with FLOX correspond to the non-recombined alleles and Δ to the recombined alleles. (**c**) Pictures of one-month-old mice of different genotypes: 1, *Cebpa*$^{fl/+}$;*Cebpb*$^{fl/+}$;K14-Cre$^{tg/+}$, 2, *Cebpa*$^{fl/fl}$;*Cebpb*$^{+/+}$;K14-Cre$^{tg/+}$, 3, *Cebpa*$^{fl/+}$;*Cebpb*$^{fl/fl}$;K14-Cre$^{tg/+}$, 4, *Cebpa*$^{fl/fl}$;*Cebpb*$^{fl/+}$;K14-Cre$^{tg/+}$. Note that the presence of only one allele of C/EBPα or C/EBPβ in the epidermis rescues the EDKO lethal phenotype and that these mice seem normal. (**d**) Graph showing weight loss of the EDKO ($n = 4$), compared with the controls ($n = 8$) before death of EDKO newborn pups by dehydration within 5–8 h. Graphs shows pup weight, compared with initial weight. The weight of the EDKO pups was significantly different from that of the control pups at all measured time-points ($P < 10^{-6}$). Results are shown as means. (**e**) X-gal penetration test[49] in newborn EDKO and control mice after 55 h of incubation. Note that only open areas (around eyes, umbilical cord, nails) are stained by X-gal. After overnight incubation no staining was observed. (**f**) Taqman Q-PCR of *Cebpa* and *Cebpb* (normalized to HPRT) in newborn epidermis. Results are shown as mean ± s.e.m. of the relative mRNA level, with control set to 1 (*$P < 0.0002$; $n = 4$ for each genotype). Controls, white bars; EDKO, black bars. (**g**) Q-PCR of newborn epidermis total RNA tested for genes downregulated in EDKO epidermis. Results are shown as mean ± s.e.m. of relative mRNA (**$P < 0.0001$; $n = 4$ for each genotype). Controls, white bars; EDKO, black bars. (**h**) Brightfield images of haematoxylin and eosin-stained skin sections of EDKO and control newborn pups. Scale bars, 20 μm.

ΔNp63 isoforms are the most prevalent[7,24]; however, in EDKO mice, suprabasal expression of ΔNp63, corresponding to the expanded K14$^+$ cell population, was observed (Fig. 4e). Although we could not demonstrate direct regulation of the *Trp63ΔN* promoter or miR-203 levels[25] by C/EBPs (R.L. and C.N, unpublished results), we observed that *N4bp1*, which encodes an inhibitor of the E3-ligase Itch[26] required for ΔNp63 degradation in keratinocytes[27], was upregulated in EDKO epidermis, whereas *Itch* expression was less altered (Fig. 4f).

Knock-in analysis of C/EBP functions in IFE keratinocytes

The above results clearly show that C/EBPα and β coordinate the cell cycle arrest of basal keratinocytes, loss of basal cell markers, and the onset of suprabasal gene expression. However, it was not clear whether this occurred through a single molecular function or through multiple, independent mechanisms. To address this question, we exploited the fact that a single intact allele of either *Cebpa* or *Cebpb* is sufficient to rescue the EDKO phenotype. This allowed mutational analysis of

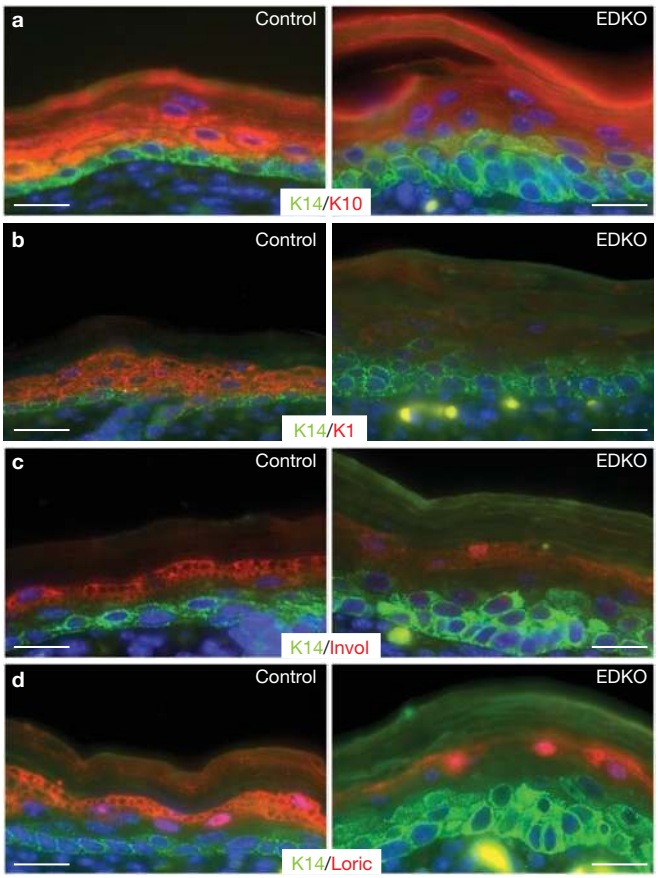

Figure 3 Differentiation defects in C/EBPα/C/EBPβ EDKO newborn pups. (**a**–**d**) Immunofluorescence microscopy was performed on skin sections of *Cebpa*$^{fl/fl}$; *Cebpb*$^{fl/fl}$ (Control) and *Cebpa*$^{fl/fl}$;*Cebpb*$^{fl/fl}$;K14-Cre$^{tg/+}$ (EDKO) newborn mice. Colour-coding is according to secondary antibodies and is marked on each frame. Nuclei were counterstained with DAPI (blue). Scale bars, 20 μm. At least 6 mice were analysed for each genotype. Panels show co-staining for keratin14/keratin10/DAPI (**a**), keratin14/keratin1/DAPI (**b**), keratin14/Involucrin/DAPI (**c**) and keratin14/Loricrin/DAPI (**d**).

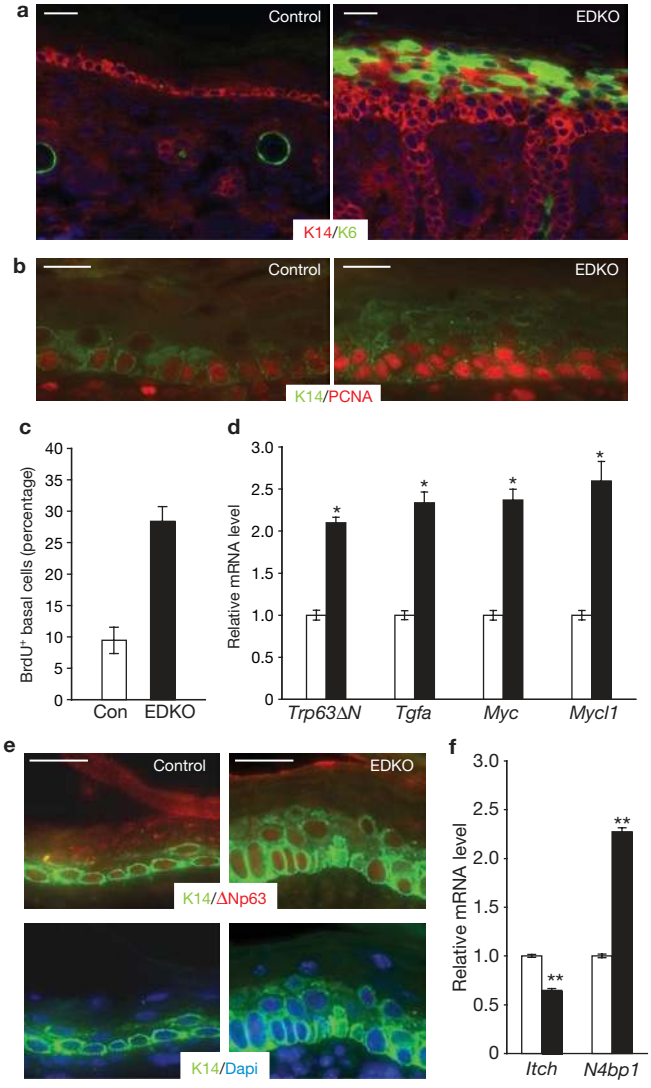

Figure 4 EDKO epidermis is hyperproliferative. (**a**, **b**) Immunofluorescence microscopy was performed on skin sections of *Cebpa*$^{fl/fl}$;*Cebpb*$^{fl/fl}$ (Control) and *Cebpa*$^{fl/fl}$;*Cebpb*$^{fl/fl}$;K14-Cre$^{tg/+}$ (EDKO) newborn mice. Colour-coding is according to secondary antibodies and is marked on each frame. Scale bars, 20 μm. (**c**) Histogram representing the percentage of BrdU incorporation in basal keratinocytes of EDKO and control epidermis. Results are shown as mean ± s.d.; control, $n = 4$; EDKO, $n = 5$. A significant difference ($P < 5 \times 10^{-6}$) between the control and EDKO mice was observed. (**d**) Q-PCR for *Trp63ΔN*, *Tgfa*, *Myc* and *Mycl1* on total RNA from control (white bars) and EDKO (black bars) newborn mouse epidermis. Results are shown as mean ± s.e.m. of relative mRNA level with the control set to 1 ($^{*}P < 10^{-4}$; $n = 4$ for each genotype) (**e**) Immunofluorescence microscopy was performed on skin sections of *Cebpa*$^{fl/fl}$;*Cebpb*$^{fl/fl}$ (Control) and *Cebpa*$^{fl/fl}$;*Cebpb*$^{fl/fl}$;K14-Cre$^{tg/+}$ (EDKO, right panels) newborn mice. Colour-coding is according to secondary antibodies and is marked on each frame. Upper panels show keratin 14/ΔNp63 co-staining, lower panels keratin 14/DAPI co-staining. Scale bars: 20 μm. (**f**) Q-PCR for *Itch* and *N4bp1* on total RNA from control (white bars) and EDKO (black bars) newborn mouse epidermis. Results are shown as mean ± s.e.m. of relative mRNA level with the control set to 1 ($^{**}P < 10^{-6}$; $n = 4$ for each genotype in triplicate).

C/EBPα by replacing a single conditional *Cebpa* allele in EDKO mice with either a control knock-in (WT) allele, or *Cebpa* alleles carrying knock-in point mutations that disable E2F interaction (BRM2 mutation, which causes mutations in residues shared between C/EBPα and -β[28]) or DNA binding (K313 duplication or KK mutation); this mutation disables both C/EBPα DNA binding and E2F repression (Supplementary Information, Fig. S3e–h).

As expected, newborn mice carrying a single wild-type *Cebpa* allele (*Cebpa*$^{WT/fl}$;*Cebpb*$^{fl/fl}$;K14-Cre$^{tg/+}$; wild-type mice) showed normal epidermal morphology. By contrast, both BRM2 mice (*Cebpa*$^{BRM2/fl}$;*Cebpb*$^{fl/fl}$;K14-Cre$^{tg/+}$) and KK mice (*Cebpa*$^{KK/fl}$;*Cebpb*$^{fl/fl}$;K14-Cre$^{tg/+}$) had shiny skin that was similar to the EDKO phenotype (Supplementary Information, Fig. S2c–f). KK IFE showed a lack of stratum granulosum and stratum corneum maturation and parakeratosis, similarly to EDKO IFE, whereas BRM2 IFE showed an intermediate phenotype (Supplementary Information, Fig. S2g). Epidermis from newborn KK and BRM2 mice both showed expanded K14/K5 expression. The delay and decrease in K1/K10 expression was similar in EDKO and KK IFE, whereas BRM2 mice showed earlier and stronger K1/K10 expression, compared with EDKO mice, giving rise to K14^{+}K10^{+} suprabasal cells (Figs 5a, b; Supplementary Information, Fig. S3c). Although loricrin was downregulated in both BRM2 and KK mutants (Fig. 5c), involucrin expression was observed in BRM2, but not KK IFE (Figs 5d), consistent with the intermediate phenotype of the BRM2 epidermis.

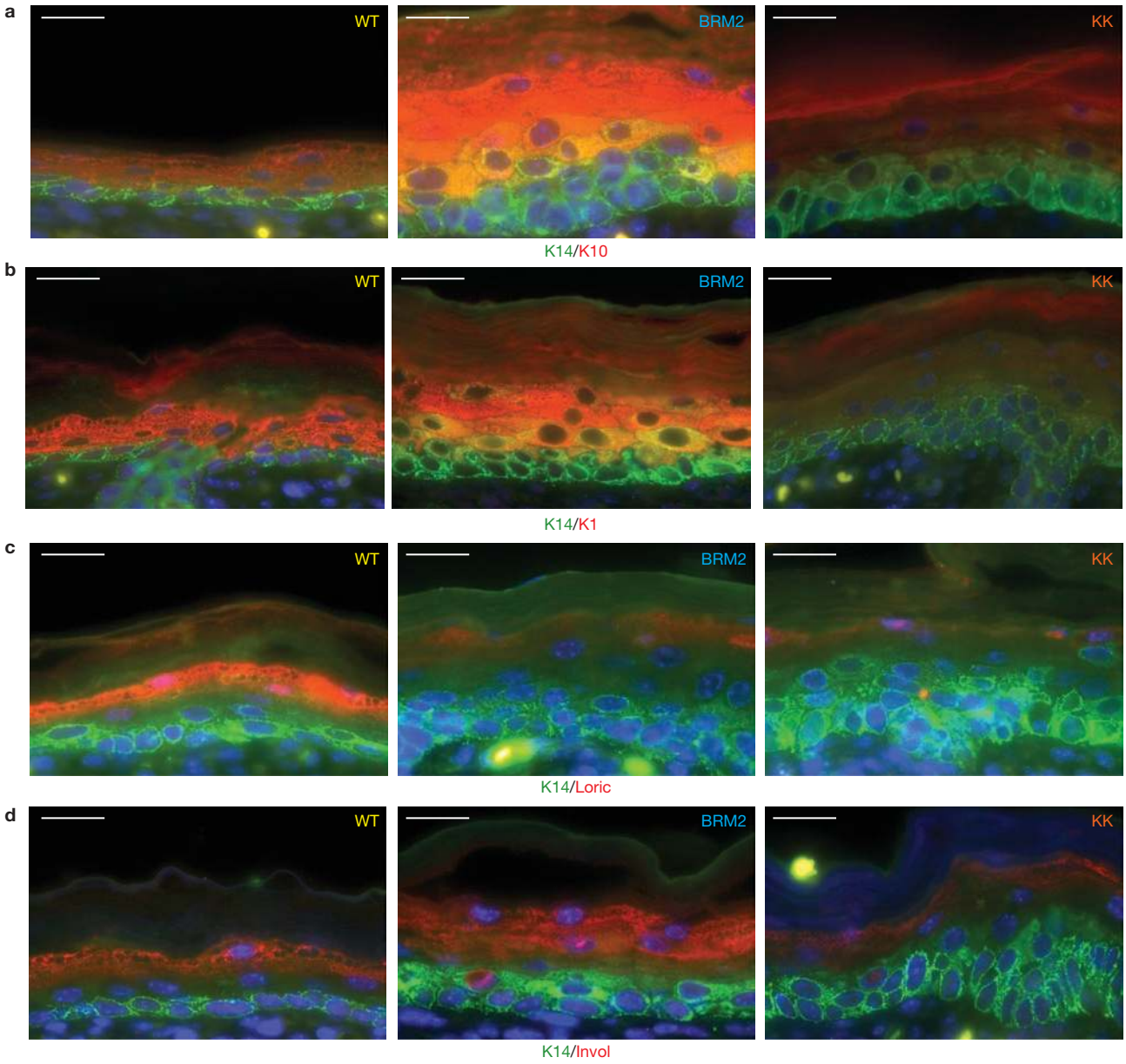

Figure 5 Genetic analysis of C/EBPα functions required for keratinocyte differentiation. (**a**–**d**) Immunofluorescence microscopy was performed on skin sections of *Cebpa*$^{fl/WT}$;*Cebpb*$^{fl/fl}$;K14-Cre$^{tg/+}$ (WT) *Cebpa*$^{fl/BRM2}$;*Cebpb*$^{fl/fl}$;K14-Cre$^{tg/+}$ (BRM2) and *Cebpa*$^{fl/KK}$;*Cebpb*$^{fl/fl}$;K14-Cre$^{tg/+}$ (KK) newborn mice. Colour-coding is according to secondary antibodies and is marked on each frame; nuclei were counterstained with DAPI (blue). Scale bars, 20 μm. Analysis was performed on 3 mice of each genotype. Panels show co-staining for keratin14/keratin10/DAPI (**a**), keratin14/keratin1/DAPI (**b**) keratin14/Loricrin/DAPI (**c**) keratin14/Involucrin/DAPI (**d**).

PCNA expression was ubiquitous in basal keratinocytes and expanded to suprabasal cells in both BRM2 and KK epidermis, compared with WT (Fig. 6a). BrdU incorporation revealed the same increase in basal cell proliferation in KK epidermis as in EDKO mice (~30% labelling index). BRM2 basal keratinocytes showed a lower proliferation rate (~20% labelling index; Fig. 6b; Supplementary Information, Fig. S3d). Loss of E2F repression may therefore not fully account for the increased proliferation in EDKO epidermis. Indeed, *Tgfa*, *Myc* and *Mycl1* mRNAs were fully upregulated only in the KK epidermis (Fig. 6c). As both E2F activity and ΔNp63 positively regulate basal cell proliferation, we investigated whether the increased proliferation of KK, compared with BRM2 basal cells, correlated with p63 expression. We found that ΔNp63 levels were increased in basal cells in KK, compared with WT and BRM2 epidermis, and that basal layer restriction of p63 expression was lost in KK, but not BRM2 mice (Fig. 6d). *Trp63* mRNA was induced in the KK epidermis (Fig. 6e), indicating upregulation at the transcriptional level. This correlated with specific upregulation of *N4bp1* in the KK genotype; no deregulation of *Itch* expression was observed (Fig. 6f).

Gene expression profiling reveals stemness control by C/EBPα/β

Given the essential role for p63 in maintaining self-renewal in the epidermis[12], the expansion of *Trp63*/ΔNp63 expression seen in the absence of C/EBPα/β suggested deregulation of stem/progenitor cell homeostasis. To identify genes deregulated by loss of C/EBP function, we performed

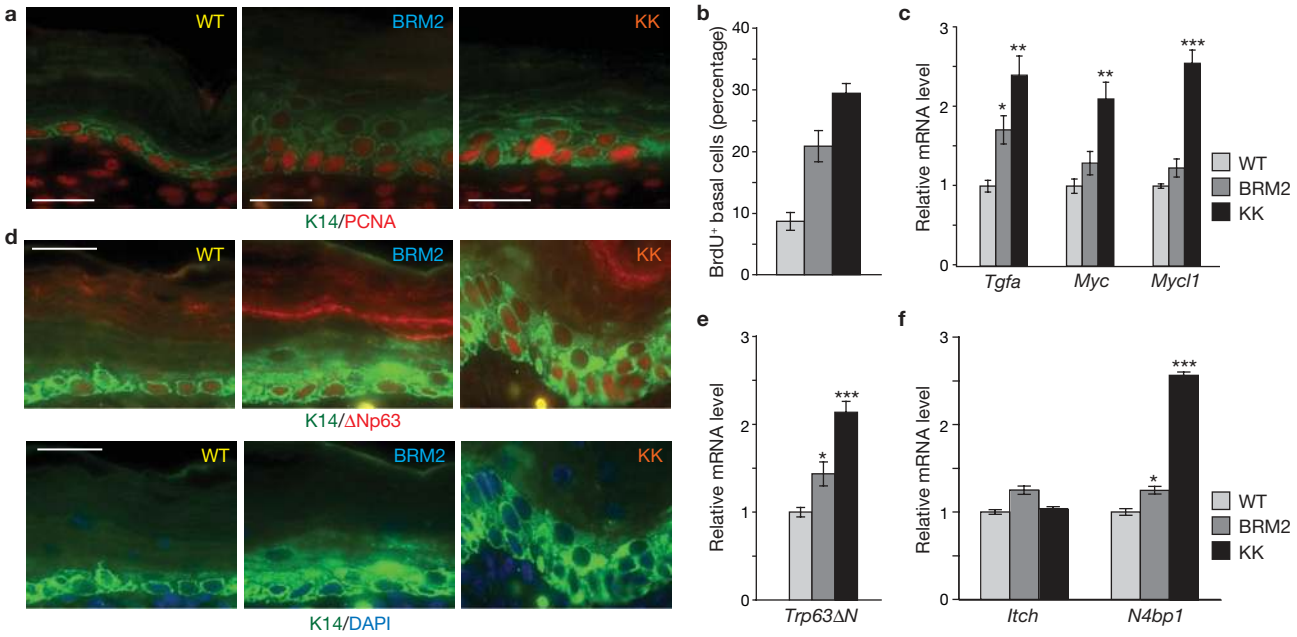

Figure 6 Regulation of gene expression and proliferation by specific C/EBP functional domains. (**a**) Immunofluorescence microscopy for K14 and PCNA staining was performed on skin sections from WT, BRM2 and KK newborn mice. Colour-coding is according to secondary antibodies and is marked on each frame. Scale bars, 20 μm. (**b**) Histogram showing the percentage of BrdU incorporation in basal keratinocytes of WT, BRM2 and KK epidermis. Results are shown as mean ± s.d., $n = 3$ for each phenotype. Significant differences between WT and BRM2 mice, WT and KK mice, or BRM2 and KK mice were observed ($P = 0.3 \times 10^{-4}$, 2×10^{-7} and 7.4×10^{-3}, respectively). (**c**) Q-PCR for *Tgfa*, *Myc*, *Mycl1* on total RNA from newborn WT, BRM2 and KK mouse epidermis. Results are shown as mean ± s.e.m. of relative mRNA level, WT = 1 (*P <0.05; **P <0.001; ***P <10^{-4}; $n = 3$ for each genotype). (**d**) Immunofluorescence microscopy for K14 and ΔNp63 was performed on skin sections of newborn WT, BRM2 and KK mice. Colour-coding is according to secondary antibodies and is marked on each frame. Scale bars, 20 μm. (**e**) Q-PCR for *Trp63*ΔN expression on total RNA from newborn WT, BRM2 and KK mouse epidermis. Results are shown as mean ± s.e.m. of relative mRNA level, WT = 1(*P < 0.05; ***P <10^{-4}; $n = 3$ for each genotype). (**f**) Q-PCR for *Itch* and *N4BP1* on total RNA from newborn WT, BRM2 and KK mouse epidermis. Results are shown as mean ± s.e.m. of relative mRNA level, WT = 1 (*P <0.05; ***P <10^{-4}; $n = 3$ for each genotype in triplicate. Colour-coding of the histogram bars is indicated in panel.

global gene profiling of EDKO, KK, BRM2 and control epidermis (including hair follicles, HFs; Supplementary Information, Table S1). To examine whether genes associated with a stem cell phenotype were enriched in the mutants, we identified several gene sets previously described as characteristic for embryonic, haematopoietic, neuronal or epithelial stem cell populations. Using gene set enrichment analysis (GSEA)[29], a high proportion of these signatures (34/54 or 63%) was enriched in EDKO epidermis, with a significant proportion enriched in KK (10/54 or 18.5%) and few signatures enriched in BRM2 (2/54 or 3.7%) epidermis (Fig. 7a; Supplementary Information, Table S2). As an example, a common embryonic stem cell signature defined by three different studies was highly enriched in EDKO epidermis (P <0.001; Fig. 7b). Interestingly, although promoters of leading edge genes were not enriched in C/EBP binding sites, compared with a random gene set, a significant enrichment of Myc/Max binding sites was observed (Supplementary Information, Table S3). The signature types upregulated in EDKO and KK epidermis were similar; however, the more prominent enrichment in EDKO epidermis indicates that stem cell signature suppression by C/EBPs is partially DNA-binding independent, possibly relying on protein–protein interaction. No specific markers have been identified to date that would allow determination of whether the IFE stem cell compartment is expanded in EDKO mice. However, we did observe that Sox9, normally restricted to HF bulge stem or progenitor cells[30,31], was ectopically expressed in mutant IFE, both basally and suprabasally, (Figs 7c, d), correlating with its increased mRNA expression (Supplementary Information, Table S1). Also, adult HF bulge stem cells are maintained in a quiescent state by nuclear NFATc1 (ref. 32), as observed in newborn control skin (Fig. 7c). However, NFATc1 was cytoplasmic in EDKO HFs, with the remaining NFATc1 localized to the cytoplasm (Fig. 7c). In both EDKO and KK epidermis, NFATc1 was cytoplasmic, whereas in BRM2 epidermis, nuclear localization was preserved (Figs 7c, d). Together, these results indicate that the C/EBP DNA binding activity, but not C/EBP-mediated E2F repression, is required for nuclear NFATc1 localization in (and, by inference, quiescence of) presumptive bulge stem cells (PBSCs).

At postnatal day (P) 0, C/EBPα and C/EBPβ are expressed in basal and suprabasal $K14^+$ HF cells and presumptive $K14^-$ matrix cells (Supplementary Information, Fig. S4a). At the P4 stage (where additional differentiation markers are expressed), co-staining with AE15 an AE13, labelling the trychohyalin layer of IRS and the hairshaft cuticle/upper cortical layer respectively, showed that C/EBPβ and, to a lesser extent, C/EBPα, are also expressed in these differentiated HF layers as well as in the matrix and basal and suprabasal ORS, as previously reported[33]. C/EBPα was present in the dermal papilla (Supplementary Information, Fig. S4b, c). In addition, C/EBPα and C/EBPβ were expressed in NFATc1-positive PBSCs (Fig. 8a; Supplementary Information, Fig. 4e, f). Co-staining for NFATc1 and Ki67 in P0 PBSCs showed that cells expressing nuclear NFATc1 were 50–70% quiescent (defined as $Ki67^-$; Fig. 8b,c; see Supplementary Fig. S4e-g for a view of the entire HF online). Loss of C/EBPα and β led to complete loss of nuclear NFATc1 and a significant decrease in quiescence (80% $Ki67^+$ PBSCs). A single *Cebpa* wild-type allele was sufficient to maintain the

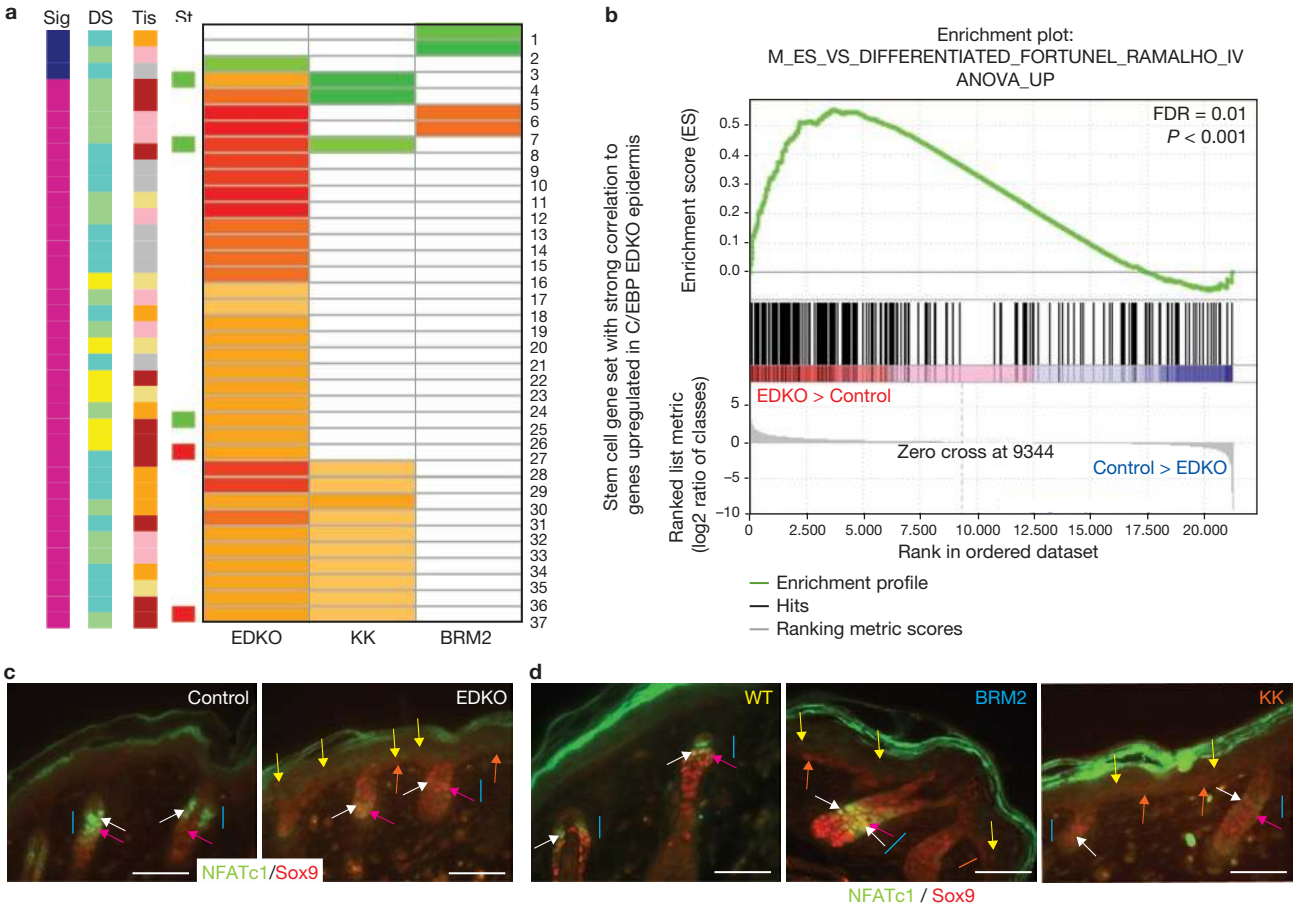

Figure 7 C/EBPα/β restrict stem cell gene signatures. (**a**) Heatmap representation of the stem cell signatures differentially enriched in the C/EBP epidermis mutants with an FDR <0.25. Gene sets enriched in the mutant and in the control are red and green, respectively. The colour intensity is inversely proportional to the FDR, and insignificant FDRs are white. On the left of the heatmap, the coloured columns reflect the biological source/status of the signature: stemness (Sig), developmental stage (DS), tissue (Tis) or cell state (St). In the Sig column, pink and dark blue show stem or anti-stem cell signatures, respectively. In the DS column, yellow is for signatures shared between developmental stages/tissues, light green for embryonic stem cell-like signatures (ES or fetal stem cells), turquoise for adult stem cell signatures. In the Tis column, light yellow is for signatures derived from multiple tissues, orange for epithelial, light pink for ES, red for haematopoietic, grey for neuronal stem cell signatures. In the St column, green and red are for proliferative and quiescent stem cell signatures, respectively. The numbers to the right of the heatmap refer to gene set IDs listed in Supplementary Information, Table S2. (**b**) Example of an enrichment plot of a stem cell signature gene set from GSEA analysis comparing mutant (EDKO) versus control gene expression profiles. Detailed results are found in Supplementary Information, Table S2. (**c**) Immunofluorescence microscopy was performed on skin sections of *Cebpa*$^{fl/fl}$;*Cebpb*$^{fl/fl}$ (Control) and *Cebpa*$^{fl/fl}$;*Cebpb*$^{fl/fl}$;K14-Cre$^{tg/+}$ (EDKO) newborn mice. Colour-coding is according to secondary antibodies. Panels show NFATc1/Sox9 co-staining. Blue bars mark PBSCs; white arrows point to NFATc1-positive PBSCs, dark pink arrows to Sox9-positive stem cell or early progenitors, orange and yellow arrows to Sox9 basal and suprabasal-positive IFE keratinocytes in mutant epidermis, respectively. Green staining in cornified layers is non-specific. Scale bars, 50 μm. (**d**) Immunofluorescence microscopy was performed on skin sections of newborn WT (left panel), BRM2 (middle panel) and KK (right panel) mice. Panels show NFATc1/Sox9 co-staining as in **c**. Labelling of figure as in **c**. Scale bars, 50 μm.

quiescent phenotype and nuclear NFATc1. Knock-in mutagenesis showed that loss of C/EBPα DNA binding, but not loss of E2F repression, delocalized NFATc1 and increased cell cycle activity (Fig. 8b,c; Supplementary Information, Fig. S4g). The proportion of quiescent PBSCs observed in this analysis is lower than that reported at P4 (ref. 32). When comparing Ki67, NFATc1 and C/EBPα expression at P0 and P4 we observed that the increased quiescence of NFATc1-positive PBSCs at P4 was accompanied by increase in C/EBPα expression (Fig. 8d, e). C/EBPα/β are thus required for nuclear localization of NFATc1 in PBSCs and consequent inhibition of PBSC proliferation, and upregulation of C/EBPα may contribute to the observed postnatal decrease in proliferation leading to a highly quiescent state. Also Sox9 was co-expressed with C/EBPα and β in the HF with higher levels of C/EBPα/β expression observed at the upper boundary of the Sox9 expression domain (Supplementary Information, Fig. S4d).

DISCUSSION

The combined epidermal loss of C/EBPα and β disrupted commitment of basal cells to the spinous layer phenotype: the K5/K14^{+} cell population was expanded to suprabasal layers, and K1/K10 expression delayed and decreased. The K10 promoter has been reported to be directly activated by both C/EBPα and β[34], and K10 expression is slightly reduced in C/EBPβ-deficient mouse epidermis[20]. However, consistent with our observation that a single allele of *Cebpa* or *Cebpb* is sufficient for normal epidermal differentiation, no disruption of commitment or terminal differentiation was observed in C/EBPβ-deficient epidermis[20]. The failure to upregulate K10, therefore, probably arises because of a requirement for direct promoter activation by C/EBP, as the BRM2 mutant (which retains DNA binding) activates K10 expression *in vivo*, whereas the DNA binding-defective KK mutant does not. A similar pattern was seen for

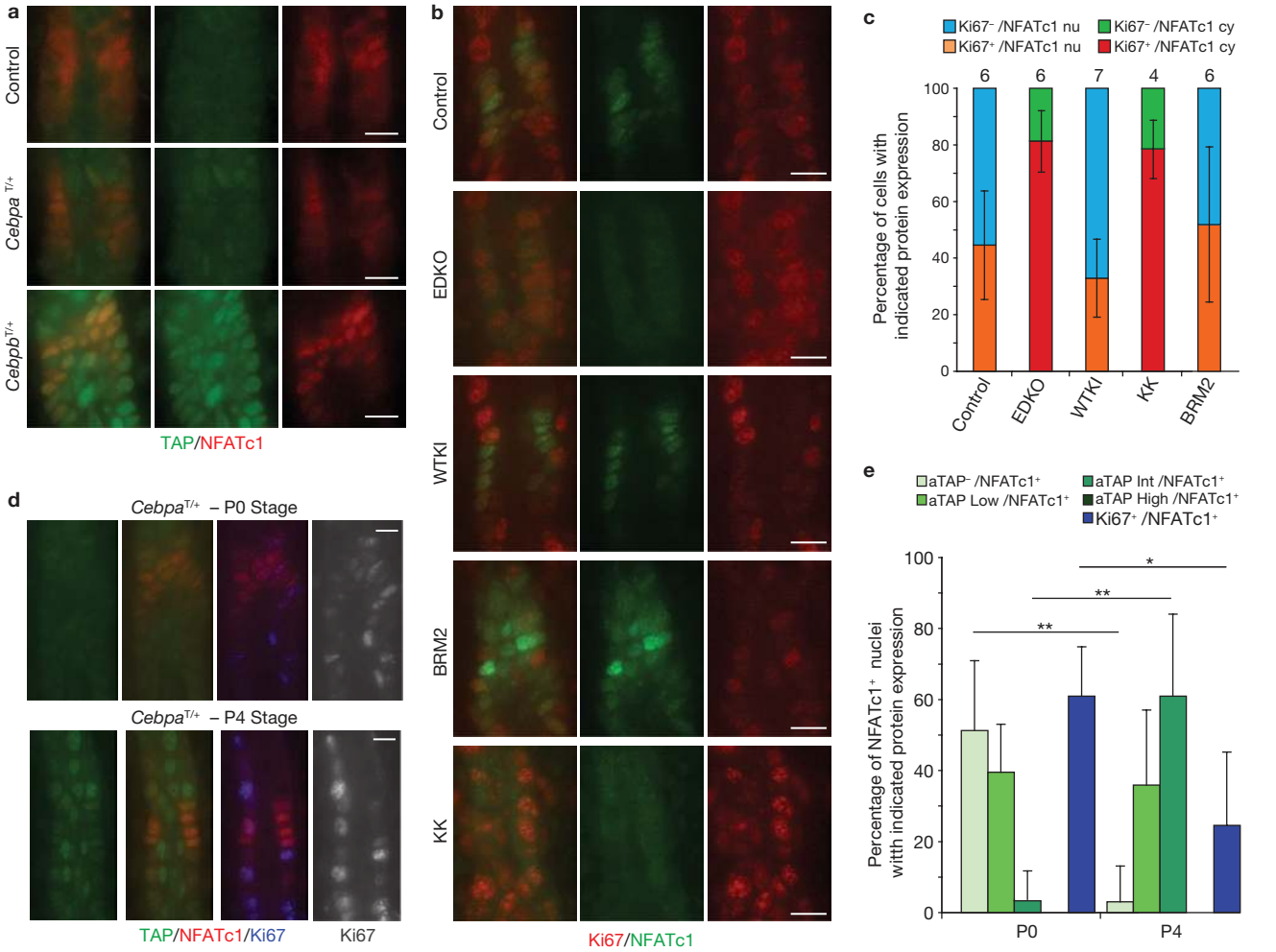

Figure 8 C/EBPα and β induce NFATc1-mediated HF stem cell quiescence. (**a**) Immunofluorescence microscopy was performed on skin sections of newborn wild-type (Control), *Cebpa*$^{T/+}$ and *Cebpb*$^{T/+}$ knock-in mice. Pictures were taken around the NFATC1-positive PBSCs area. From right to left, panels show NFATc1 staining, TAP staining and TAP/NFATc1 overlay. Scale bars, 10 μm. (**b**) Immunofluorescence microscopy was performed on skin sections of *Cebpa*$^{fl/fl}$;*Cebpb*$^{fl/fl}$ (Control), *Cebpa*$^{fl/fl}$;*Cebpb*$^{fl/fl}$;K14-Cre$^{tg/+}$ (EDKO), *Cebpa*$^{fl/WT}$;*Cebpb*$^{fl/fl}$;K14-Cre$^{tg/+}$ (WT) *Cebpa*$^{fl/BRM2}$;*Cebpb*$^{fl/fl}$;K14-Cre$^{tg/+}$ (BRM2) and *Cebpa*$^{fl/KK}$;*Cebpb*$^{fl/fl}$;K14-Cre$^{tg/+}$ (KK) newborn mice. Pictures were taken around the NFATc1-positive PBSCs area. This area is defined by nuclear NFATc1 staining for control, WT and BRM2 mutants, and by cytoplasmic NFATc1 staining for EDKO and KK mutants. From right to left, panels show staining for Ki67, NFATc1 and NFATc1/Ki67 overlay. Scale bars, 10 μm. (**c**) Histogram showing the percentage of NFATc1-positive cells that show Ki67 co-staining (Ki67$^+$) or no Ki67 co-staining (Ki67$^-$) in the P0 PBSCs area identified by nuclear or cytoplasmic NFATc1 (NFATc1, nu and NFATc1, cy, respectively). Results are shown as percentage of NFATc1-positive PBSCs with or without Ki67 co-expression (mean ± s.d.). The number of Ki67+ in NFATc1 HF-expressing keratinocytes was significantly different in EDKO, compared with control ($P = 0.0022$; Student's *t*-test) or KK compared with WTKI control ($P = 0.0003$), but not in BRM2 versus WTKI control ($P = 0.134$). *n* values are indicated above the bars. (**d**) Immunofluorescence microscopy was performed on skin sections of *Cebpa*$^{T/+}$ knock-in mice at P0 (upper panels) and P4 stages (lower panels). From left to right, panels show TAP staining, TAP/NFATc1 overlay, NFATc1/Ki67 overlay, and Ki67 staining (greyscale) in the NFATc1-positive PBSCs area, respectively. Scale bars, 10 μm. (**e**) Histogram showing the percentage of NFATc1-positive HF keratinocytes (NFATc1$^+$) that show co-expression of either C/EBPα–TAP (green columns), or Ki67 (blue columns) at P0 and P4 stages. C/EBPα–TAP expression was divided into 4 categories: no, low, intermediate and high expression (αTAP –, αTAP Low, αTAP Int and αTAP High, respectively). Results are shown as percentage of NFATc1$^+$ nuclei with indicated protein expression (mean ± s.d.; $^*P < 2.10^{-4}$; $^{**}P < 10^{-5}$; aTAP P0, $n = 10$; aTAP, P4, $n = 11$). *n* values in **c** and **e** represent the number of hair of follicles counted from two mice.

involucrin expression. Indeed, C/EBP sites within the involucrin promoter are required for its expression *in vivo*[35]. It is not known at present which transcription factors control the ΔNp63 expression pattern *in vivo*. Here we show that C/EBPα and β have a crucial role in restricting ΔNp63 expression to basal keratinocytes, with repression of *N4bp1* as a potential mechanism. As ΔNp63 activates its own promoter[36], increased ΔNp63 stability could explain the increased *Trp63ΔN* mRNA levels.

Basal keratinocyte proliferation was markedly increased in the absence of C/EBPα/β. We found that both C/EBPα and β are expressed in the nuclei of basal cells, consistent with the increase in proliferation being a cell-intrinsic effect of C/EBP depletion. C/EBPs have been proposed to inhibit the cell cycle by several mechanisms, including E2F repression[37]. The latter is a property shared by C/EBPα and β, and requires basic region residues conserved between the two isoforms[28]. Loss of C/EBPα-E2F interaction was sufficient to increase basal cell proliferation. Epidermal ablation of *Rb1* and *Rbl1* (encoding pRb and p107, respectively) also results in failure of keratinocytes to downregulate K14 on migration into suprabasal layers, leading to co-expression of K14 and

K10[5]. These results are all consistent with C/EBPs and Rb family members cooperating to regulate the cell cycle exit before commitment to differentiation[38]. However, although loss of C/EBP-mediated E2F repression increased basal cell proliferation, further loss of DNA binding led to an additional increase. As *Trp63* promotes the proliferation of basal keratinocytes[12,13], ΔNp63 upregulation may contribute to the observed increase in proliferation. Recently it was found that combined loss AP-2α and AP-2γ led to a severe defect in terminal keratinocyte differentiation, associated with downregulation of C/EBPα and C/EBPβ expression[39]. Our results are consistent with decreased C/EBP expression in suprabasal keratinocytes underlying the differentiation defects observed in the absence of AP-2α/γ.

Epidermal depletion of C/EBPα and β led to upregulation of gene expression associated with diverse stem cell populations. This suggests that C/EBPs may act also in the epidermis to restrict stem cell function. A role for C/EBPs in suppressing stem cell gene expression could also provide a basis for their ability to modulate epidermal cancer susceptibility[19,21,40], in particular, as ES cell-like gene expression signatures are found in human epithelial cancers[41,42]. *In vitro* ES cell signatures were induced by *Myc* overexpression in keratinocytes[41]. *Myc* and *Mycl1* are both upregulated in EDKO and KK epidermis, consistent with the known ability of C/EBPα to repress the *Myc* promoter[43], providing a mechanism by which loss of C/EBPα/β can induce ES cell signatures in keratinocytes *in vivo*. Consistent with this mechanism, upregulation of stem cell signatures occurs predominantly in the EDKO and KK genotypes, and leading edge genes of upregulated ES signatures were enriched in Myc binding sites. We found that Sox9 is ectopically expressed in C/EBP-deficient IFE. Sox9 is normally associated with HF bulge stem cells[30,44] and progenitors, and HF Sox9-derived cells contribute to the IFE replenishment following epidermal damage[30]. As Sox9 expression is a characteristic of basal cell carcinomas and adnexal-derived skin neoplasms[31], it may be one of the genes acting downstream of C/EBPs in tumour suppression. NFATc1, which is required in its nuclear form to maintain PBSC quiescence[32], is depleted from PBSC nuclei in EDKO and KK (but not BRM2) epidermis, whereas Sox9 is also expressed ectopically in the BRM2 mutant. PBSC proliferation is increased only in EDKO and KK mice where NFATc1 is localized in the cytoplasm, demonstrating that C/EBPα and β suppress PBSC proliferation by enforcing nuclear translocation of NFATc1, a mechanism distinct from that operating in the IFE where control of C/EBP-mediated proliferation is largely dependent on E2F repression.

In the EDKO epidermis cornified envelope proteins (loricrin, involucrin, filaggrin) and genes encoding proteins involved in lipid (*Sts*) and profilaggrin processing (*Casp14*) fail to express normally. Loss of lipid biosynthesis, Sprr2a (a loricrin crosslinker[4]), Sts and Casp14 have all been correlated to loss of the water barrier[45–48]. Combined loss of C/EBPα and β affects all of these aspects of stratum corneum formation, and the loss of barrier function is therefore consistent with the molecular phenotype. However, loss of the water barrier was not accompanied by increased keratinocyte proliferation in *Gata3*, *Klf4* and *Casp14* null epidermis, suggesting that the increased proliferation of EDKO basal keratinocytes is not a consequence of the water barrier dysfunction, particularly as it occurs in E18.5 embryos.

In summary, C/EBPα and β have redundant, essential functions in the epidermis. C/EBPα and β modulate the expression of key molecules essential for epidermal barrier formation. In addition, C/EBPα and β are involved through E2F inhibition in the coupling between cell cycle exit and the commitment of epidermal differentiation of keratinocytes, in a process that also involves the direct activation of differentiation-specific promoters and downregulation of ΔNp63 and stem cell signature genes.

METHODS

Methods and any associated references are available in the online version of the paper at http://www.nature.com/naturecellbiology/.

Note: Supplementary Information is available on the Nature Cell Biology website.

ACKNOWLEDGEMENTS

This work was supported by the European Commission (EuroStemCell integrated project, EuroCSC STREP). R.L. was the recipient of a Marie Curie Fellowship; S.G. was supported by a fellowship from the Spanish Ministry of Research; O.B. was supported by an HFSP postdoctoral fellowship.

AUTHOR CONTRIBUTIONS

R.L. J.P. and C.N. designed experiments; R.L. performed analysis; S.G. performed biochemical characterization of KK and C/EBP-TAP knock-ins, R.L., O.B. and O.E. generated mouse lines; S.M. performed bioinformatics analysis; A.B.M.-C. and E.K. provided technical assistance; R.L. and C.N. wrote the manuscript.

COMPETING INTERESTS

The authors declare that they have no competing financial interest.

Published online at http://www.nature.com/naturecellbiology/
Reprints and permissions information is available online at http://npg.nature.com/reprintsandpermissions/

1. Fuchs, E. & Horsley, V. More than one way to skin. *Genes Dev.* **22,** 976–985 (2008).
2. Jones, P. H., Simons, B. D. & Watt, F. M. Sic transit gloria: farewell to the epidermal transit amplifying cell? *Cell Stem Cell* **1,** 371–381 (2007).
3. Blanpain, C. & Fuchs, E. Epidermal stem cells of the skin. *Annu. Rev. Cell Dev. Biol.* **22,** 339–373 (2006).
4. Candi, E., Schmidt, R. & Melino, G. The cornified envelope: a model of cell death in the skin. *Nature Rev. Mol. Cell Biol.* **6,** 328–340 (2005).
5. Ruiz, S. *et al.* Unique and overlapping functions of pRb and p107 in the control of proliferation and differentiation in epidermis. *Development* **131,** 2737–2748 (2004).
6. Thalmeier, K., Synovzik, H., Mertz, R., Winnacker, E. L. & Lipp, M. Nuclear factor E2F mediates basic transcription and trans-activation by E1a of the human MYC promoter. *Genes Dev.* **3,** 527–536 (1989).
7. Rounbehler, R. J., Schneider-Broussard, R., Conti, C. J. & Johnson, D. G. Myc lacks E2F1's ability to suppress skin carcinogenesis. *Oncogene* **20,** 5341–5349 (2001).
8. Yang, A. *et al.* p63 is essential for regenerative proliferation in limb, craniofacial and epithelial development. *Nature* **398,** 714–718 (1999).
9. Mills, A. A. *et al.* p63 is a p53 homologue required for limb and epidermal morphogenesis. *Nature* **398,** 708–713 (1999).
10. Lechler, T. & Fuchs, E. Asymmetric cell divisions promote stratification and differentiation of mammalian skin. *Nature* **437,** 275–280 (2005).
11. Lee, H. & Kimelman, D. A dominant-negative form of p63 is required for epidermal proliferation in zebrafish. *Dev. Cell* **2,** 607–616 (2002).
12. Senoo, M., Pinto, F., Crum, C. P. & McKeon, F. p63 is essential for the proliferative potential of stem cells in stratified epithelia. *Cell* **129,** 523–536 (2007).
13. Truong, A. B., Kretz, M., Ridky, T. W., Kimmel, R. & Khavari, P. A. p63 regulates proliferation and differentiation of developmentally mature keratinocytes. *Genes Dev.* **20,** 3185–3197 (2006).
14. Nguyen, B. C. *et al.* Cross-regulation between Notch and p63 in keratinocyte commitment to differentiation. *Genes Dev.* **20,** 1028–1042 (2006).
15. Blanpain, C., Lowry, W. E., Pasolli, H. A. & Fuchs, E. Canonical notch signaling functions as a commitment switch in the epidermal lineage. *Genes Dev.* **20,** 3022–3035 (2006).
16. Oh, H. S. & Smart, R. C. Expression of CCAAT/enhancer binding proteins (C/EBP) is associated with squamous differentiation in epidermis and isolated primary keratinocytes and is altered in skin neoplasms. *J. Invest. Dermatol.* **110,** 939–945 (1998).
17. Maytin, E. V. & Habener, J. F. Transcription factors C/EBPα, C/EBPβ, and CHOP (Gadd153) expressed during the differentiation program of keratinocytes *in vitro* and *in vivo*. *J. Invest. Dermatol.* **110,** 238–246 (1998).
18. Di-Poi, N., Desvergne, B., Michalik, L. & Wahli, W. Transcriptional repression of peroxisome proliferator-activated receptor β/δ in murine keratinocytes by CCAAT/enhancer-binding proteins. *J. Biol. Chem.* **280,** 38700–38710 (2005).
19. Nerlov, C. The C/EBP family of transcription factors: a paradigm for interaction between gene expression and proliferation control. *Trends Cell Biol.* **17,** 318–324 (2007).
20. Zhu, S. *et al.* C/EBPβ modulates the early events of keratinocyte differentiation involving growth arrest and keratin 1 and keratin 10 expression. *Mol. Cell. Biol.* **19,** 7181–7190 (1999).

21. Loomis, K. D., Zhu, S., Yoon, K., Johnson, P. F. & Smart, R. C. Genetic ablation of CCAAT/enhancer binding protein alpha in epidermis reveals its role in suppression of epithelial tumorigenesis. *Cancer Res.* **67,** 6768–6776 (2007).
22. Lee, Y. H., Sauer, B., Johnson, P. F. & Gonzalez, F. J. Disruption of the *c/ebp* α gene in adult mouse liver. *Mol. Cell Biol.* **17,** 6014–6022 (1997).
23. Hafner, M. *et al.* Keratin 14 Cre transgenic mice authenticate keratin 14 as an oocyte-expressed protein. *Genesis* **38,** 176–181 (2004).
24. Laurikkala, J. *et al.* p63 regulates multiple signalling pathways required for ectodermal organogenesis and differentiation. *Development* **133,** 1553–1563 (2006).
25. Yi, R., Poy, M. N., Stoffel, M. & Fuchs, E. A skin microRNA promotes differentiation by repressing 'stemness'. *Nature* **452,** 225–229 (2008).
26. Oberst, A. *et al.* The Nedd4-binding partner 1 (N4BP1) protein is an inhibitor of the E3 ligase Itch. *Proc. Natl Acad. Sci. USA* **104,** 11280–11285 (2007).
27. Rossi, M. *et al.* The E3 ubiquitin ligase Itch controls the protein stability of p63. *Proc. Natl Acad. Sci. USA* **103,** 12753–12758 (2006).
28. Porse, B. T. *et al.* E2F repression by C/EBPα is required for adipogenesis and granulopoiesis *in vivo*. *Cell* **107,** 247–258 (2001).
29. Subramanian, A. *et al.* Gene set enrichment analysis: a knowledge-based approach for interpreting genome-wide expression profiles. *Proc. Natl Acad. Sci. USA* **102,** 15545–15550 (2005).
30. Nowak, J. A., Polak, L., Pasolli, H. A. & Fuchs, E. Hair follicle stem cells are specified and function in early skin morphogenesis. *Cell Stem Cell* **3,** 33–43 (2008).
31. Vidal, V. P., Ortonne, N. & Schedl, A. SOX9 expression is a general marker of basal cell carcinoma and adnexal-related neoplasms. *J. Cutan. Pathol.* **35,** 373–379 (2008).
32. Horsley, V., Aliprantis, A. O., Polak, L., Glimcher, L. H. & Fuchs, E. NFATc1 balances quiescence and proliferation of skin stem cells. *Cell* **132,** 299–310 (2008).
33. Bull, J. J. *et al.* Contrasting expression patterns of CCAAT/enhancer-binding protein transcription factors in the hair follicle and at different stages of the hair growth cycle. *J. Invest. Dermatol.* **118,** 17–24 (2002).
34. Maytin, E. V. *et al.* Keratin 10 gene expression during differentiation of mouse epidermis requires transcription factors C/EBP and AP-2. *Dev. Biol.* **216,** 164–181 (1999).
35. Crish, J. F., Gopalakrishnan, R., Bone, F., Gilliam, A. C. & Eckert, R. L. The distal and proximal regulatory regions of the involucrin gene promoter have distinct functions and are required for *in vivo* involucrin expression. *J. Invest. Dermatol.* **126,** 305–314 (2006).
36. Antonini, D. *et al.* An autoregulatory loop directs the tissue-specific expression of p63 through a long-range evolutionarily conserved enhancer. *Mol. Cell. Biol.* **26,** 3308–3318 (2006).
37. Schuster, M. B. & Porse, B. T. C/EBPα: a tumour suppressor in multiple tissues? *Biochim. Biophys. Acta* **1766,** 88–103 (2006).
38. Sebastian, T., Malik, R., Thomas, S., Sage, J. & Johnson, P. F. C/EBPβ cooperates with RB:E2F to implement Ras(V12)-induced cellular senescence. *EMBO J.* **24,** 3301–3312 (2005).
39. Wang, X., Pasolli, H. A., Williams, T. & Fuchs, E. AP-2 factors act in concert with Notch to orchestrate terminal differentiation in skin epidermis. *J. Cell Biol.* **183,** 37–48 (2008).
40. Zhu, S., Yoon, K., Sterneck, E., Johnson, P. F. & Smart, R. C. CCAAT/enhancer binding protein-beta is a mediator of keratinocyte survival and skin tumorigenesis involving oncogenic Ras signaling. *Proc. Natl Acad. Sci. USA* **99,** 207–212 (2002).
41. Wong, D. J. *et al.* Module map of stem cell genes guides creation of epithelial cancer stem cells. *Cell Stem Cell* **2,** 333–344 (2008).
42. Ben-Porath, I. *et al.* An embryonic stem cell-like gene expression signature in poorly differentiated aggressive human tumors. *Nature Genet.* **40,** 499–507 (2008).
43. Johansen, L. M. *et al.* c-Myc is a critical target for c/EBPα in granulopoiesis. *Mol. Cell. Biol.* **21,** 3789–3806 (2001).
44. Vidal, V. P. *et al.* Sox9 is essential for outer root sheath differentiation and the formation of the hair stem cell compartment. *Curr. Biol.* **15,** 1340–1351 (2005).
45. de Guzman Strong, C. *et al.* Lipid defect underlies selective skin barrier impairment of an epidermal-specific deletion of Gata-3. *J. Cell Biol.* **175,** 661–670 (2006).
46. Segre, J. A., Bauer, C. & Fuchs, E. Klf4 is a transcription factor required for establishing the barrier function of the skin. *Nature Genet.* **22,** 356–360 (1999).
47. Elias, P. M. *et al.* Basis for abnormal desquamation and permeability barrier dysfunction in RXLI. *J. Invest. Dermatol.* **122,** 314–319 (2004).
48. Denecker, G. *et al.* Caspase-14 protects against epidermal UVB photodamage and water loss. *Nature Cell Biol.* **9,** 666–674 (2007).
49. Hardman, M. J., Sisi, P., Banbury, D. N. & Byrne, C. Patterned acquisition of skin barrier function during development. *Development* **125,** 1541–1552 (1998).

METHODS

Mouse strains. K14-Cre transgenic mice[23], and the conditional[22], WTKI and BRM2 (ref. 28) *Cebpa* alleles have been described previously. The *Cebpa* KK allele (containing a duplication of Lys 313), the *Cebpb* conditional allele, as well as the knock-in alleles encoding C/EBPα–TAP and C/EBPβ–TAP knock-in mice, which contain a TAP tag[50] inserted after the last amino acid of C/EBPα and C/EBPβ, respectively, were generated as described previously[28]. Details of constructs and genotyping are given below. Strains were maintained on a mixed C57BL/6-129/Ola background. All mouse procedures were approved by the EMBL Monterotondo Ethical Committee.

C/EBPβ conditional knockout mice. The *Eco*RI flanked sequence containing a LoxP site was obtained by annealing the following oligomers: 5′-AAT TCA TAA CTT CGT ATA GCA TAC ATT ATA CGA AGT TAT-3′ and 5′-AAT TCA TAA CTT CGT ATA ATG TAT GCT ATA CGA AGT TAT-3′. The annealed product was subcloned into an *Eco*RI linearized NSRI plasmid, which carries a *Not*I–*Sal*I fragment of the mouse genomic clone of C/EBPβ with an ectopic *Eco*RI restriction site 11 bp before the start codon site. The *Not*I–*Sal*I fragment was then transferred into the pTV-flox-C/EBPβ targeting construct (NSRI and pTV-flox-C/EBPβ plasmid were from A. Leutz, Max-Delbrück Center, Berlin, Germany), which already contains a floxed neomycine resistance cassette in the 3′-UTR of C/EBPβ for ES cell selection. To check the correct orientation of the introduced LoxP site, XL1-blue bacteria expressing thermosentive Cre recombinase were transformed with the obtained product and their recombined plasmid DNA was analysed for the absence of a 1.9 kb fragment on *Not*I/*Sal*I digestion. The obtained targeted construct pTV-LoxP-C/EBPβ-NeoFlox was then linearized by *Sca*I digestion before transfection into ES cells.

Four hundred and fifty neomycin-resistant ES clones were picked and analysed for homologous recombination of the *Cebpb* locus by *Eco*RI digestion of the DNA and Southern blotting hybridization using a 700-bp external probe. This probe was obtained by an *Eco*RI–*Xba*I digestion of the 9N1R plasmid (provided by E. Sterneck, National Cancer Institute, Frederick, MD, USA). Five clones were positives and two clones were injected into blastocysts to generate chimaeric mice. Germline transmission of the C/EBPβ Flox allele was obtained and C/EBPβ Flox homozygous mice were obtained by breeding C/EBPβ Flox heterozygous mice. The genotype of these mice is obtained by Southern blotting using the same approach as that used for the ES cell screening.

TAP knock-in mice. The pSVKeo-FRT-CTAP-FRT-EYFP basic construct was obtained as follows (sequence available on request): The C-TAP cassette was PCR amplified using the following oligomers: 5′-GTTGGCGCGCCTCTAGAATTCTGCAGTTAACATCCATGGAAAAGAGAAGATGGAAAAAGAATTTCATAGCCG-3′ and 5′-GCGCGTCGACGCTTCAGGTTGACTTCCCCGCAGAGTTCGCGTCTACT-3′. The PCR product was subcloned into *Asc*I/*Sal*I digested pSVKeoX1 targeting plasmid, which allows the introduction into pSVKeoX1 of the CTAP cassette preceded by a multiple cloning site including *Asc*I, *Xba*I, *Eco*RI, *Pst*I and *Hpa*I restriction sites, and followed by a STOP codon and *Sal*I cloning site. The following oligomers 5′-GAAGTTCCTATACTTTCTAGAGAATAGGAACTTCCC-3′ and 5′-GGGAAGTTCCTATTCTCTAGAAAGTATAGGAACTTC-3′ were annealed and introduced into the *Hpa*I restriction site, allowing the introduction of an FRT site situated upstream of the CTAP cassette. The resulting plasmid was called pSVKeo-FRT-CTAP. The EYFP cassette was PCR amplified using the following primers: 5′-GTGCTCGAGAAGTTCCTATTCTCTAGAAAGTATAGGAACTTCAATGGTGAGCAAGGGCGAGGAG-3′ and 5′-GTGGTCGACTTACTTGTACAGCTCGTCCATGC–3′. The PCR product digested by *Sal*I and *Xho*I was subcloned into *Sal*I restricted pSVKeo-FRT-CTAP, which introduces respectively an additional FRT site and an EYFP encoding cassette downstream of the C-TAP cassette.

To engineer a C/EBPα–TAP targeting construct, the homologous arm of 500 bp derived from the unique exon of C/EBPα and 3'UTR were sub-cloned into *Xba*I–*Pst*I and *Xho*I–*Not*I sites of pSVKeo-FRT-CTAP-FRT-EYFP basic construct, respectively. The *Xba*I–*Not*I fragment containing homologous *Cebpa* arms, TAP tag and pGK/neo cassette was excised and electroporated together with a genomic murine *Cebpa* clone to allow ET recombination[51]. The resulting targeting vector was linearized and electroporated into E14.1 ES cells. Two hundred clones were picked and expanded. Southern blot analysis of *Sca*I digested genomic DNA, using a 900-bp probe located outside the targeting construct identified 2% of the clones as correctly targeted by the appearance of a 14.5-kb fragment, whereas a 9.5-kb fragment was present in the non-targeted allele. Two clones were injected into C57Bl/6 blastocysts and the resulting chimaeras were bred for germline transmission.

To engineer a C/EBPβ–TAP targeting construct, the homologous arm of 500 bp derived from the exon of C/EBPβ and the 3′UTR were subcloned into the *Asc*I–*Eco*RI and *Xho*I–*Not*I sites, respectively, of pSVKeo-FRT-CTAP-FRT-EYFP basic construct. The *Asc*I–*Not*I fragment containing homologous *Cebpb* arms, TAP tag and pGK/neo cassette was excised and electroporated together with a genomic murine C/EBPβ to allow ET recombination[51]. The resulting targeting vector was linearized and electroporated into E14.1 ES cells. Two hundred neomycin-resistant clones were picked and expanded. Southern blot analysis of *Hinc*II-digested genomic DNA, using a 900-bp probe located outside the targeting construct identified 2 clones as correctly targeted by the appearance of a 4-kb fragment, whereas a 10-kb fragment was present in non-targeted allele. Two clones were injected into C57Bl/6 blastocysts and the resulting chimeras were bred for germline transmission.

Genotyping of C/EBPα–TAP and C/EBPβ–TAP mice. C/EBPα–TAP mice were genotyped by PCR using the following oligomers: 5′-GGTCAAGGCCATGGGCAACTGCGCG–3′; 5′-GGAAAGTCTCTCGGTCTCAAGGAGAAAC-3′ and 5′-GTGCAGATGAACTTCAGG-3′. C/EBPβ–TAP mice were genotyped by PCR using the following oligomers: 5′-GCAGCTGCCCGAGCCGCTGCTGGCCTC-3′; 5′-CATCTTTAAGGTGATTACTCAGGGC-3′-and 5′-GTGCAGATGAACTTCAGG 3′.

PCR amplification for C/EBPα-TAP and C/EBPβ-TAP genotyping was performed by PCR using the following conditions: initial denaturation (94 °C, 4 min), 35 cycles of denaturation (94 °C, 40 s), annealing (55 °C, 45 s) and elongation (72 °C, 1 min), and final elongation (72 °C, 5 min). Wild-type *Cebpa* and *Cebpa* TAP alleles yield 270-bp and 827-bp PCR products, respectively. Wild-type *Cebpb* and *Cebpb* TAP alleles yield 370-bp and 927- bp PCR products, respectively.

C/EBPα KK knock-in mice. The C/EBPα KK knock-in construct was generated using a previously described targeting strategy[28]. C/EBPα WTKI, C/EBPα BRM2 and C/EBPα KK knock-in mice were genotyped by PCR followed by a BssHII restriction enzyme digestion. The oligomers and PCR amplification conditions were respectively: 5′-CGCTGGTGATCAAACAAGAG 3' and 5' CTCGTTGCTGTTCTTGTCCA 3′, Initial denaturation (94 °C – 4 min), 30 cycles of denaturation (94 °C, 30 s), annealing (55 °C, 30 s) and elongation (72°C, 1.2 min), and final elongation (72 °C, 10 min). Then, one fifth of the PCR amplified product was digested for 3 h at 50 °C with *BssH*II restriction enzyme. A *BssH*II site is present in mouse, but absent in rat C/EBPa, allowing us to distinguish the knock-in allele from the wild type allele. PCR products from homozygous C/EBPα knock-ins therefore yield an unique 400-bp band, whereas wild-type mice by 290-bp and 110-bp bands, and heterozygous knock-in mice by a 400-bp, a 290-bp and a 110-bp bands.

PCR of conditional floxed and deleted *Cebpa* and *Cebpb* alleles. C/EBPα conditional floxed allele (control) and K14-Cre mediated deletion allele (EDKO) were evaluated by PCR using the following primers and PCR conditions: 5′-CCACTCACCGCCTTGGAAAGTCACA 3′; 5′-CCGCGGCTCCACCTCGTAGAAGTCG 3′; and 5′-GTCCTGCAGCCAGGCAGTGTCC 3′, Initial denaturation (97 °C, 2 min), 35 cycles of denaturation (94 °C, 30 s), annealing (60 °C, 30 s) and elongation (72 °C, 30 s), and final elongation (72 °C, 10 min). The C/EBPa conditional floxed allele gives a 355-bp product, and K14-Cre mediated C/EBPα-deletion allele a 560-bp product.

C/EBPβ conditional floxed allele (control) and K14-Cre mediated deletion allele (EDKO) were also evaluated by PCR using oligomers and conditions as follows:

5′-CCTTATAAACCTCCCGCTC 3′; 5′-CTCACGTAACCGTAGTCG 3′; 5′-CCCTCAACTCTCACTAATGCG 3′, Initial denaturation (95 °C, 5 min), 5 cycles of denaturation (95 °C, 1 min), annealing (50 °C, 1 min) and elongation (72 °C, 1 min), followed by 40 cycles of denaturation (95 °C, 1 min), annealing (53 °C, 1 min) and elongation (72 °C, 1 min) and final elongation (72 °C, 5 min). The C/EBPβ conditional floxed allele gives a 470-bp product, and K14-Cre mediated C/EBPβ-deletion allele a 580-bp product.

Histology and immunostainings. Pictures of newborn mice were taken with a videomicroscope (Leica MZ12) equipped with a Leica DC500 digital camera. X-gal

DOI: 10.1038/ncb1960

List of antibodies/dilutions

Protein	Antibody type	Dilution	Company
Keratin 14	Mouse monoclonal	1/400	Neomarkers
Keratin 14	Rabbit polyclonal	1/2000	Covance
Keratin 5	Rabbit polyclonal	1/2000	Covance
Keratin 10	Rabbit polyclonal	1/1000	Covance
Keratin 10	Mouse monoclonal	1/200	DakoCytomation
Keratin 1	Rabbit polyclonal	1/2000	Covance
Keratin 6	Rabbit polyclonal	1/500	Covance
Loricrin	Rabbit polyclonal	1/500	Covance
Involucrin	Rabbit polyclonal	1/500	Covance
PCNA	Mouse monoclonal	1/200	Biosource
ΔNp63	Goat polyclonal	1/200	Santa Cruz Biotechnology
anti-BrdU	Mouse monoclonal	1/500	Chemicon International
Ki67	Rabbit polyclonal	1/150	Dianova
Ki67	Rat monoclonal	1/50	DakoCytomation
NFATc1	Mouse monoclonal	1/200	Santa Cruz Biotechnology
Sox9	Rabbit polyclonal	1/100	Santa Cruz Biotechnology
Sox9	Goat Polyclonal	1/150	Santa Cruz Biotechnology
AE13	Mouse monoclonal	1/10	Dr. TT Sun, NY
AE15	Mouse monoclonal	1/10	Dr. TT Sun, NY
Biotinylated anti-mouse IgGs	Horse polyclonal	1/300	Vector Laboratories
Streptavidin-Alexa488		1/1000	InVitrogen
Streptavidin-Alexa594		1/1000	InVitrogen

and Toluidine Blue permeability tests were performed essentially as described previously[49]. Briefly, newborn mice were rinsed in PBS, immersed in X-gal solution, pH4.5 at 30 °C for up to 55 h or in Toluidine Blue solution for 5 min at room temperature, washed twice in PBS for 1–2 min and photographed. Newborn mouse back skin samples were fixed in 4% PFA, then dehydrated and embedded in paraffin. Rehydrated 5-μm sections were stained with haematoxylin and eosin for histology or subjected to antigen retrieval R-Buffer AG using a Retriever 2100 (PickCell Laboratories) for 20 min. Before overnight incubation at 4 °C with primary antibodies diluted in PBST (PBS+0.05% Tween 20) and 0.25% cold water fish skin gelatin, sections were blocked for 1 h at room temperature in goat or horse normal serum (10% in PBST; Vector). Antibodies and dilutions are listed in the table below.

For TAP staining, sections were blocked in PBS containing 3% BSA and 0.05% Tween 20, then incubated with primary antibodies which were a rabbit non-immune rabbit serum (NIRS; 1/100; a gift from R. Gareus, EMBL, Monterotondo, Italy) and anti-K10 (or anti-K14, or anti-NFATc1) mouse monoclonal antibody, or anti-Ki67 rat monoclonal antibody, or anti-Sox9 goat polyclonal antibody.

After three washes, Alexa coupled secondary antibodies were applied. Slides were washed 3 times in PBST and mounted in Vectashield with DAPI (Vector Laboratories).

NFATc1 was detected using a two steps method: briefly, the mouse monoclonal anti-NFATc1 primary antibody was recognized by 1 hour incubation with biotinylated anti-mouse IgGs, which were subsequently detected using Streptavidin Alexa 488 (or Streptavidin Alexa 594 for the costaining with TAP) at 1/1000 dilution for 1 hour at room temperature.

All data were collected at 630X magnification with a Leica DMR fluorescent microscope equipped with a Leica DC500 digital camera. Except for Figs 7c, d, 8a, b, d, and for Supplementary Information, Fig. S3d and Fig. S4, photos of fluorescent stainings show only IFE as published previously[25]. Pictures in Figs 7c, d show stainings within all skin compartments as indicative of sectioning quality in accordance with EMBL/CIEMAT standards.

According the primary antibodies used, secondary antibodies Donkey anti-rabbit Alexa 594, Donkey anti-rabbit Alexa 488, Donkey anti-mouse Alexa 488, Donkey anti-mouse Alexa 594, Donkey anti-goat Alexa 594, Donkey anti-rat Alexa 594 (Molecular Probes), DyLight 649 conjugated Donkey anti-rat (Jackson Laboratories) were diluted to 1:1000 in PBST.

BrdU incorporation and quantification. For BrdU incorporation, pregnant females at E18.5 of embryonic development were injected with BrdU (200 μg g^{-1}) and killed after 2 h. Back skin of E18.5 embryos were fixed immediately in 4% paraformaldehyde (PFA). Back skin sections were stained as described above with anti-BrdU and anti-K14 antibodies with a 2M HCl pretreatment. For each sample (3–5 pups per genotype), 200–300 interfollicular basal keratinocytes from at least 2 different sections were counted.

Sample preparation for microarrays and real-time PCR. Trunk skin from newborn pups was incubated for 1 h at 4°C with a 2.5% trypsin solution without calcium (Gibco). Epidermis was separated from the dermis, washed in PBS without calcium and magnesium (Gibco) and snap-frozen in liquid nitrogen. Total RNA was extracted with TRIzol reagent (Invitrogen Life Technologies) and 25 μg of total RNA was purified on RNAeasy columns (Qiagen).

Quantitative real time PCR was performed as described previously[52] using SYBR Green JumpStart Taq Ready Mix kit (Sigma) (primer sequences listed in the table below). All experiments were done in duplicate using 3–4 different samples for each genotype, and ubiquitin expression levels used to normalize between samples.

TaqMan probes (Applied Biosystems) were used to evaluate the RNA expression levels for Cebpa (Mm00514283_s1 probe), Cebpb (Mm00843434_s1 probe), Itch (Mm00492683_m1 probe) and N4bp1 (Mm00772994_m1 probe) normalized to the expression level of HPRT (Mm00446968_m1 probe) using the TaqMan Universal Master Mix, No AmpErase UNG (Applied Biosystems).

Total RNA was hybridized to Affymetrix MOE430 2.0 microarrays after 1 round of linear amplification and analysed as described previously[53].

GSEA analysis. Pre-filtered, normalized data were tested for gene set enrichment using GSEA v2.0 (ref. 29; http://www.broad.mit.edu/gsea/). Each genotype (EDKO, KK and BRM2) was compared with the control in a separate test. Gene set characteristic of stem cells were curated from refs 54 and 55, or taken from ref. 41.

GSEA enrichment results were filtered for statistical significance using an FDR *q* value threshold of 0.25 to yield gene sets for which at least one genotype yielded a significant result. FDRs for these were plotted on a heatmap.

RT–PCR primers		
Gene	**Forward primer**	**Reverse primer**
Casp1	ACAACCACTCGTACACGTCTT	GGCAGCAAATTCTTTCACCTCTT
Casp14	CCAACCTATACGGATACCCTCC	AGTCGGGTGATCTCTTCTGTC
Sts	GGGGACAGGGTGATTGACG	TTGGGCGTGAAGTAGAAGGC
Tgm3	GCAGCACAAATCGAATTGGCA	CACAGGGTCACGACGGAAAT
Trp63	GGAAAACAATGCCCAGACTCAAT	GAGAGAGGGCATCAAAGGTGGAG
Tgfa	CACTCTGGGTACGTGGGTG	CACAGGTGATAAGAGGACAGC
Myc	GCAAGTGCTCCAGCCCCAGGTC	GCCCCAGCCAAGGTTGTGAGGTTA
Mycl1	GGGTACAGTGTGGGGGACAGAC	CCGCAGCAGCTTATAAAACACAA
Ubb1	GCAAGTGGCTAGAGTGCAGAGTAA	TGGCTATTAATTATTCGGTCTGCAT

Motif scanning analysis. Leading edge genes were taken for genesets significantly enriched in the EDKO versus WT GSEA analysis, and promoter sequences (spanning –2000 bp to +500 bp, relative to the TSS) were downloaded from ENSEMBL (v 54; NCBI M37) using BioMart. These sequences (called 'LedgeProm') were scanned for the presence of a subset of TRANSFAC motifs using the RSAT web server[56]. Motif scanning of an equal number of randomly selected genes (RandomProm) was performed in parallel. The number of unique genes having one or more matches for a given motif was normalized to input number to calculate match frequency. Statistically significant over-representation of motif matches in LedgeProm vs RandomProm was determined with a hypergeometric test.

EMSA assays. 293T cells were transfected with 1.5 μg of pcDNA1-C/EBPα WT or pcDNA1-C/EBPα KK by standard calcium phosphate procedures and nuclear extracts were prepared as described[57]. Nuclear proteins (5 μg) were preincubated for 10 min on ice in binding buffer (20 mM Tris pH 8, 75 mM KCl, 0.1 mg ml-1 BSA, 10% glycerol, 0.1 mg ml^{-1} poly[d(I-C)], 1 mM DTT and protease inhibitors cocktail from Roche). Cold competitor (250-fold excess) or 0.5 μg of antibodies (anti-C/EBPα sc-61X, anti-C/EBPβ sc-150X or anti-c-MYC sc-764X, all from Santa Cruz Biotechnology) were added and binding reactions were incubated for another 15 min on ice. ^{32}P-labelled double stranded probe SNE7 (TCGAATATTAGGACATCTTGAC) was then added (30,000 cpm) and incubation continued at room temperature for 20 min. Samples were resolved on 6% polyacrylamide gels in 0.5× TBE buffer. Gels were fixed, dried and exposed to film at –70 °C.

Western blots. Liver nuclear extracts were prepared from adult mice as described[58]. Nuclear proteins were quantified, aliquoted and 5× SDS loading buffer was added to samples. Culture cells were lysed in 1× Laemmli lysis buffer and boiled for 20 min. Approximately 100 μg of protein in50 μl) was loaded per lane, resolved on 10% SDS–PAGE gels and blotted onto PVDF membranes (Hybond-P, Amersham Biosciences). Immunoblots were blocked in 5% milk in PBST (PBS-0, 5%Tween ; Sigma) for 1 h at room temperature and incubated for 2 h with the following antibodies in 5% milk PBST: anti-C/EBPα sc-61, 1:1500; anti-C/EBPβ sc-150, 1:1500 (Santa Cruz Biotechnology); anti-α-tubulin DM 1A, 1:5000; anti-PAP (P1291), 1:2000 (Sigma). After 3 wash with PBST (10 min), blots were incubated 1 h with secondary antibodies against rabbit or mouse IgG (1:10000, Jackson Immunolaboratories) and washed again before being developed using ECL (Amersham Biosciences).

Statistical analysis. Comparison of numerical data was performed using Student's *t*-test. A hypergeometric test was used to compare occurrence of TRANSFAC motifs in promoter sets.

Microarray data. Microarray data have been deposited in the ArrayExpress database (http://www.ebi.ac.uk/microarray-as/ae/) with the accession number E-MEXP-1719.

50. Rigaut, G. *et al.* A generic protein purification method for protein complex characterization and proteome exploration. *Nature Biotechnol.* **17,** 1030–1032 (1999).
51. Zhang, Y., Buchholz, F., Muyrers, J. P. & Stewart, A. F. A new logic for DNA engineering using recombination in Escherichia coli. *Nature Genet.* **20,** 123–128 (1998).
52. Kirstetter, P., Anderson, K., Porse, B. T., Jacobsen, S. E. & Nerlov, C. Activation of the canonical Wnt pathway leads to loss of hematopoietic stem cell repopulation and multilineage differentiation block. *Nature Immunol.* **7,** 1048–1056 (2006).
53. Kirstetter, P. *et al.* Modeling of C/EBPα mutant acute myeloid leukemia reveals a common expression signature of committed myeloid leukemia-initiating cells. *Cancer Cell* **13,** 299–310 (2008).
54. Rhee, H., Polak, L. & Fuchs, E. Lhx2 maintains stem cell character in hair follicles. *Science* **312,** 1946–1949 (2006).
55. Venezia, T. A. *et al.* Molecular signatures of proliferation and quiescence in hematopoietic stem cells. *PLoS Biol.* **2,** e301 (2004).
56. Turatsinze, J. V., Thomas-Chollier, M., Defrance, M. & van Helden, J. Using RSAT to scan genome sequences for transcription factor binding sites and cis-regulatory modules. *Nature Protocols* **3,** 1578–1588 (2008).
57. Dignam, J. D., Lebovitz, R. M. & Roeder, R. G. Accurate transcription initiation by RNA polymerase II in a soluble extract from isolated mammalian nuclei. *Nucleic Acids Res.* **11,** 1475–1489 (1983).
58. Timchenko, N. A. *et al.* CCAAT/enhancer binding protein alpha regulates p21 protein and hepatocyte proliferation in newborn mice. *Mol. Cell. Biol.* **17,** 7353–7361 (1997).

nature cell biology

DOI: 10.1038/ncb1960

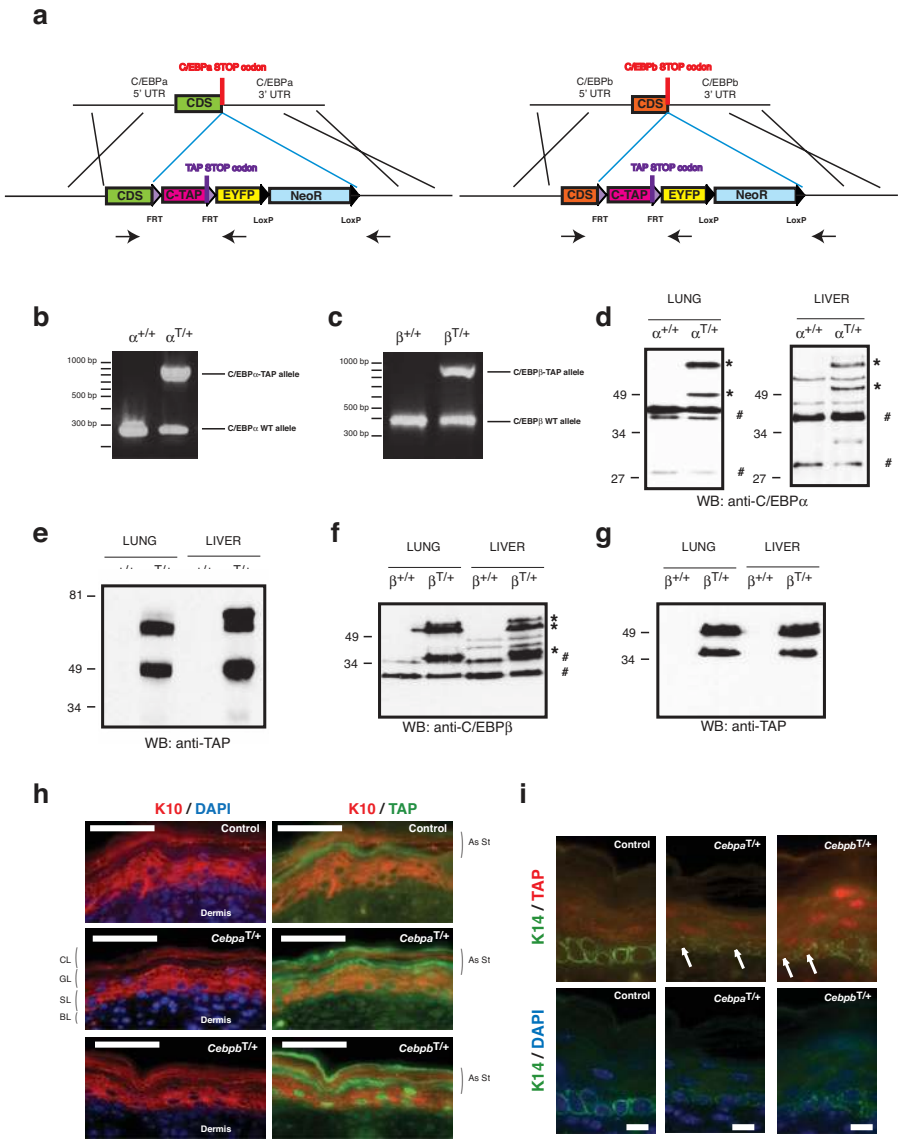

Figure S1 Generation of TAP tagged C/EBP knockins and C/EBP-TAP epidermal expression pattern. (**a**) Schematic representation of Cebpa-TAP and Cebpb-TAP knock-in alleles. The FRT-CTAPstop-FRT-EYFPstop-LoxP-NeoR-LoxP cassette is knocked-in by homologous recombination in Cebpa and Cebpb alleles instead of their respective open reading frame stop codons (red), given rise to a C/EBP-CTAP fusion protein. Arrows represent primers used for genotyping by PCR. (**b**) PCR genotype of wild type ($\alpha^{+/+}$) and Cebpa-TAP heterozygous mice ($\alpha^{T/+}$). Wild type allele: 270 bp band; Cebpa-TAP allele: 827 bp band. (**c**) PCR genotype of wild type ($\beta^{+/+}$) and Cebpb-TAP heterozygous mice ($\beta^{T/+}$). Wild type allele: 370 bp band; and Cebpb-TAP allele: 927 band. (**d**) C/EBPα immunoblot analysis of lung (left panel) and liver (right panel) proteins from 2-months old wild type ($\alpha^{+/+}$) or Cebpa-TAP heterozygous ($\alpha^{T/+}$) mice. # indicate the p42 and p30 isoforms of C/EBPα, while * indicate the p42-TAP and p30-TAP isoforms. (**e**) TAP specific immunoblot analysis of lung and liver proteins from 2-months old wild type ($\alpha^{+/+}$) or Cebpa-TAP heterozygous ($\alpha^{T/+}$) mice. (**f**) C/EBPβ immunoblot analysis of lung and liver proteins from 2-months old wild type ($\beta^{+/+}$) or Cebpb-TAP heterozygous ($\beta^{T/+}$) mice. # indicate the LIP and LAP isoforms of C/EBPβ, while * indicate LIP-TAP, LAP-TAP and LAP*-TAP isoforms. (**g**) TAP specific immunoblot analysis of lung and liver proteins from 2-months old wild type ($\beta^{+/+}$) or Cebpb-TAP heterozygous ($\beta^{T/+}$) mice. (**h**) Immunofluorescence microscopy was performed on newborn skin sections of wild–type (control), Cebpa-TAP (*Cebpa*$^{T/+}$) or Cebpb-TAP (*Cebpb*$^{T/+}$) heterozygous knockin mice. Sections were stained for TAP (green), K10 (red) and DAPI (blue). Scale bars: 50 μm. (**i**) Immunofluorescence microscopy was performed as in (h). Sections were stained for TAP (red), K14 (green) and DAPI (blue). Arrows indicate examples of K14+ basal keratinocytes expressing C/EBPα-TAP or C/EBPβ-TAP. Scale bars: 10 μm. Figure abbreviations: CDS, coding sequence; CTAP, Carboxyterminal Tandem Affinity Purification tag; EYFP, enhanced yellow fluorescent protein; NeoR, neomycin resistance cassette; UTR, untranslated region. WT, wild type; WB, western blot. BL (basal layer); SL (spinous layer); GL (granular layer); CL (cornified layer); As ST (aspecific staining).

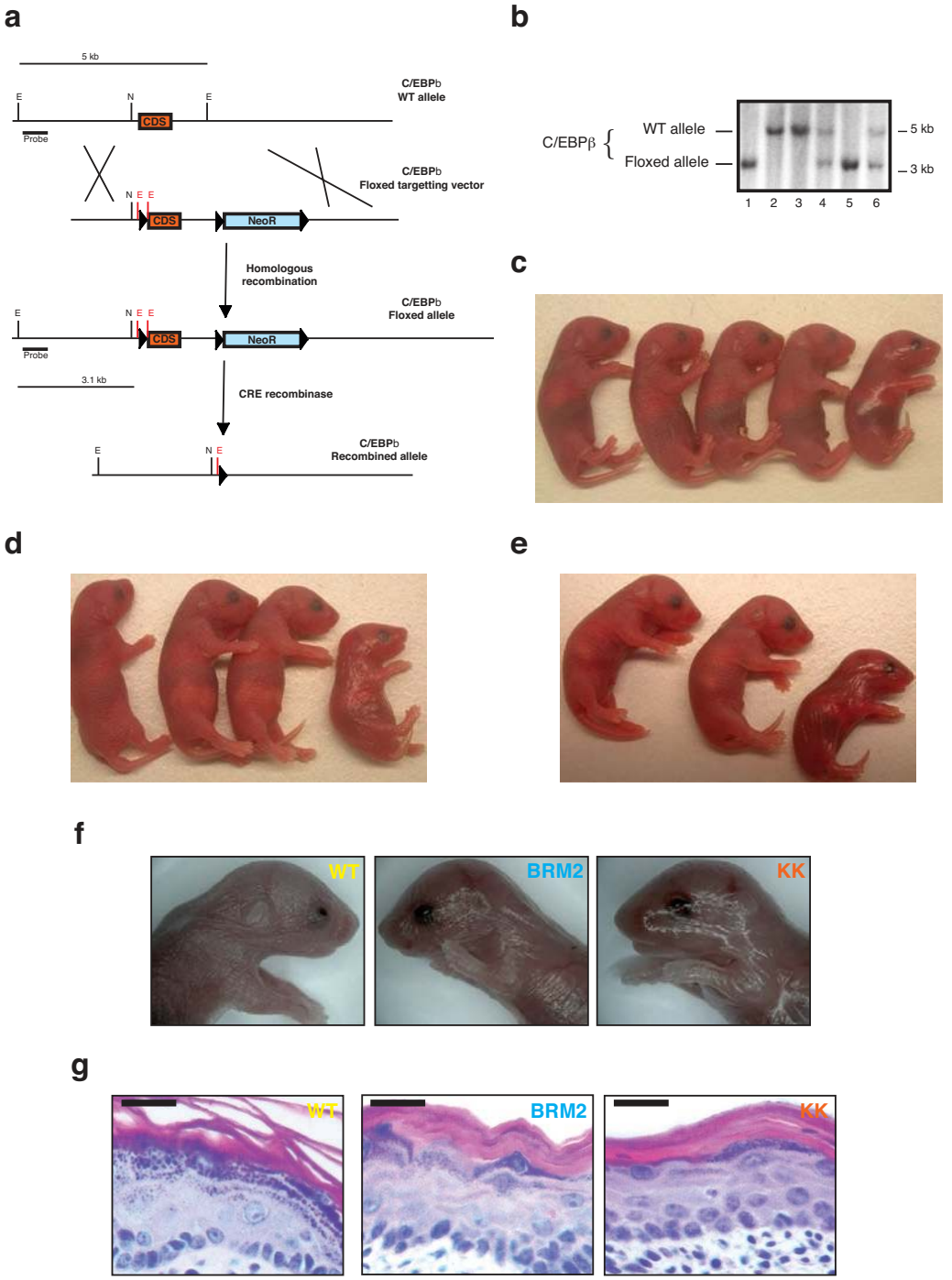

Figure S2 Generation of conditional *Cebpb* allele and Morphology of C/EBP EDKO and KI/KO epidermis. (**a**) Schematic representation of wild type *Cebpb* (WT), conditional (Floxed) and recombined *Cebpb* alleles. Abbreviations: E, EcoRI restriction site; N, NotI restriction site; CDS, coding sequence; NeoR, neomycin resistance cassette; kb, kilobase. The binding site of the probe used for Southern blot is shown. (**b**) Southern blot analysis of *Cebpb* wild type (lanes 2 & 3), *Cebpb* floxed heterozygous (lanes 4 & 6) and homozygous (lanes 1 & 5) mice. A band of 5 kb and 3.1 kb are detected in the case of *Cebpb* wild type and *Cebpb* Floxed alleles, respectively (see schematic in a). (**c**) Full size appearance of littermate newborn pups photography: From right to left *Cebpa*$^{fl/fl}$; *Cebpb*$^{fl/fl}$; K14-Cre$^{tg/+}$ (EDKO), *Cebpa*$^{fl/fl}$; *Cebpb* $^{fl/+}$; K14-Cre$^{+/+}$, C/EBPα$^{fl/KK}$; *Cebpb*$^{fl/+}$; K14-Cre$^{tg/+}$, *Cebpa*$^{fl/fl}$; *Cebpb*$^{+/+}$; K14-Cre$^{tg/+}$ and *Cebpa*$^{fl/KK}$; *Cebpb* $^{+/+}$; K14-Cre$^{tg/+}$. (**d**) Full size appearance of littermate newborn pups photography: From right to left *Cebpa*$^{fl/BRM2}$; *Cebpb*$^{fl/fl}$; K14-Cre$^{tg/+}$ (BRM2), *Cebpa*$^{fl/BRM2}$; *Cebpb*$^{fl/+}$; K14-Cre$^{tg/+}$, *Cebpa*$^{fl/BRM2}$; *Cebpb*$^{fl/+}$; K14-Cre$^{+/+}$ and *Cebpa*$^{fl/BRM2}$; *Cebpb*$^{fl/fl}$; K14-Cre$^{+/+}$. (**e**) Full size appearance of littermate newborn pups photography: From right to left *Cebpa*$^{fl/KK}$; *Cebpb*$^{fl/fl}$; K14-Cre$^{tg/+}$ (KK), *Cebpa*$^{fl/fl}$; *Cebp* $^{+/+}$; K14-Cre$^{tg/+}$ and *Cebpa*$^{fl/fl}$; *Cebpb*$^{+/+}$; K14-Cre$^{+/+}$. (**f**) Images of the general appearance of *Cebpa*$^{fl/WT}$; *Cebpb*$^{fl/fl}$; K14-Cre$^{tg/+}$ (WT control, left panel), *Cebpa*$^{fl/BRM2}$; *Cebpb*$^{fl/fl}$; K14-Cre$^{tg/+}$ (BRM2 mutant, middle panel) and *Cebpa*$^{fl/KK}$; *Cebpb*$^{fl/fl}$; K14-Cre$^{tg/+}$ (KK mutant, right panel) newborn pups. (**g**) Brightfield images of hematoxylin/eosin-stained skin sections from *Cebpa*$^{fl/WT}$; *Cebpb*$^{fl/fl}$; K14-Cre$^{tg/+}$ (WT control, left panel), *Cebpa*$^{fl/BRM2}$; *Cebpb*$^{fl/fl}$; K14-Cre$^{tg/+}$ (middle panel, BRM2) and *Cebpa*$^{fl/KK}$; *Cebpb*$^{fl/fl}$; K14-Cre$^{tg/+}$ (right panel, KK) newborn pups. Black scale bars: 20 μm.

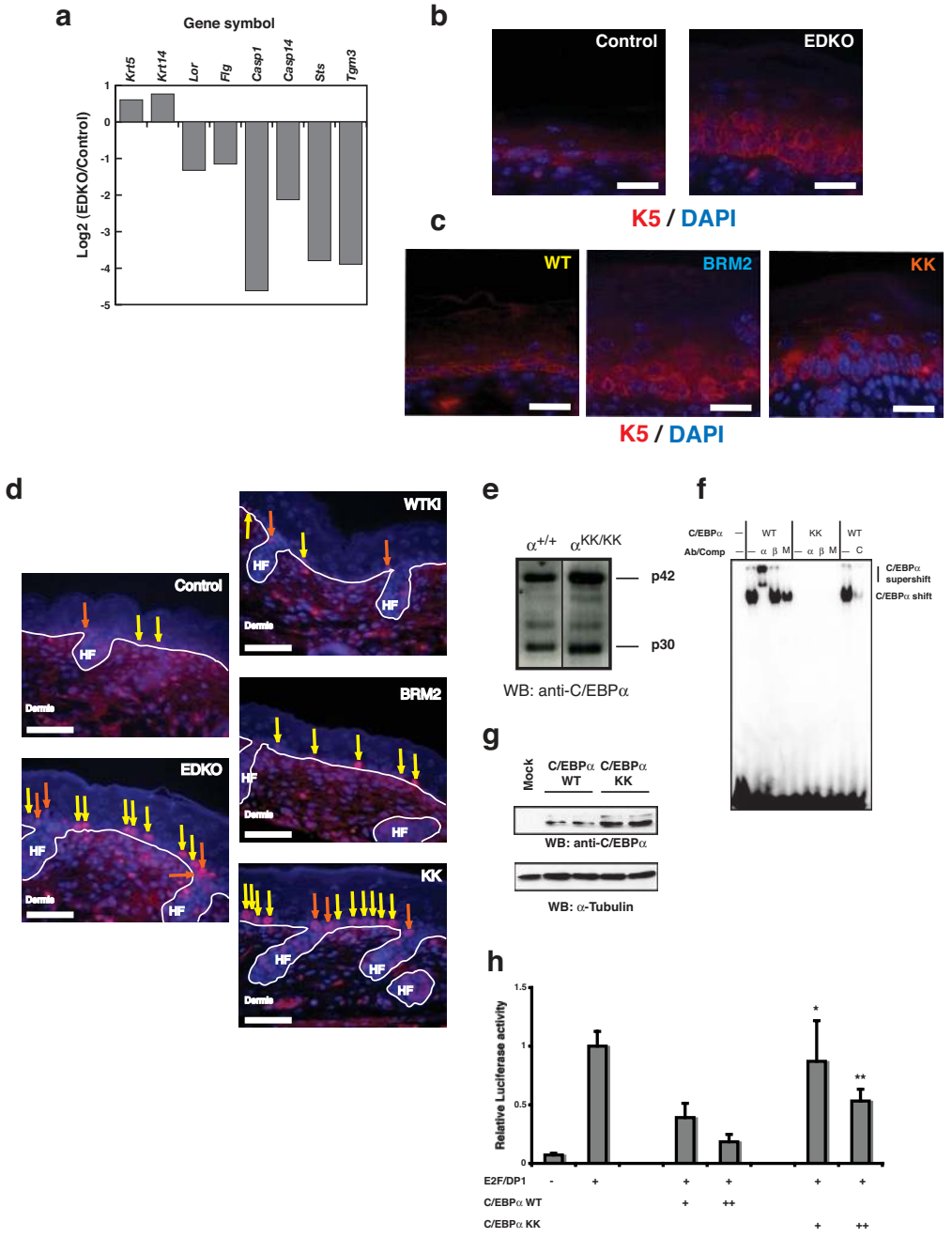

Figure S3 Expression pattern in C/EBP mutant epidermis, BrdU stainings of controls and C/EBP mutant E18.5 embryos, and characterization of C/EBPα KK mutant. (**a**) Fold change in expression for selected genes calculated as the log2 ratio of the averaged EDKO and control Affymetrix expression intensity values. (**b**) Immunofluorescence microscopy was performed on skin sections from *Cebpa*$^{fl/fl}$; *Cebpb*$^{fl/fl}$ (control, left panel) and *Cebpa*$^{fl/fl}$; *Cebpb*$^{fl/fl}$; K14-Cre$^{tg/+}$ (EDKO, right panel) newborn mice. Keratin 5/DAPI co-staining. Scale bars: 20 μm. (**c**) Immunofluorescence microscopy was performed as in (b) on skin sections from *Cebpa*$^{fl/WT}$; *Cebpb*$^{fl/fl}$; K14-Cre$^{tg/+}$ (WT panel), *Cebpa*$^{fl/BRM2}$; *Cebpb*$^{fl/fl}$; K14-Cre$^{tg/+}$ (BRM2 panel) and *Cebpa*$^{fl/KK}$; *Cebpb*$^{fl/fl}$; K14-Cre$^{tg/+}$ (KK panel) newborn mice. Scale bars: 20 μm. (**d**) Immunofluorescence microscopy was performed on skin sections from *Cebpa*$^{fl/fl}$; *Cebpb*$^{fl/fl}$ (control for EDKO, left top panel); *Cebpa*$^{fl/fl}$; *Cebpb*$^{fl/fl}$; K14-Cre$^{tg/+}$ (EDKO, left bottom panel); *Cebpa*$^{WT/fl}$; *Cebpb*$^{fl/fl}$; K14-Cre$^{tg/+}$(WTKI: control for BRM2 and KK, right top panel); *Cebpa*$^{BRM2/fl}$; *Cebpb*$^{fl/fl}$; K14-Cre$^{tg/+}$ (BRM2, right middle panel) and *Cebpa*$^{KK/fl}$; *Cebpb*$^{fl/fl}$; K14-Cre$^{tg/+}$ (KK, right bottom panel) E18.5 embryos. BrdU/DAPI co-staining. BrdU positive basal IFE keratinocytes (yellow arrows) were counted for quantification; BrdU positive keratinocytes in hair follicles (HF) or at the IFE and HF boundary (orange arrow) were not. Scale bars: 50 μm. (**e**) C/EBPα protein expression in WT and KK/KK transgenic mice. Western blotting with 14AA anti-C/EBPα antibody of nuclear extracts from embryonic livers at E14.5. (**f**) Gel Shift analysis of C/EBP binding activity in nuclear extracts (NE) from 293T transfected cells with expression vectors for WT and KK mutant C/EBPα. (**g**) C/EBPα expression levels in 293T transfected cells used in Gel Shift analysis. Upper panel: immunoblotting with anti-C/EBPα antibody; Lower panel: loading control immunobloting with α-tubulin antibody. (**h**) E2F repression activity by C/EBPα KK mutant. 293T cells were transiently transfected with p6xE2F-TATA luc reporter plasmid (100ng), CMV expression vectors for E2F-1 and DP-1 (5ng each) and increasing amounts (25 and 200ng) of WT or KK mutant C/EBPα CMV expression vectors. Values represent the average of 2 experiments each performed in triplicate, normalized to the value obtained with E2F-1+DP-1 alone. Asterisks: values significantly different from that obtained with WT C/EBPα; (*) p<0.02; (**) p=0.0001.

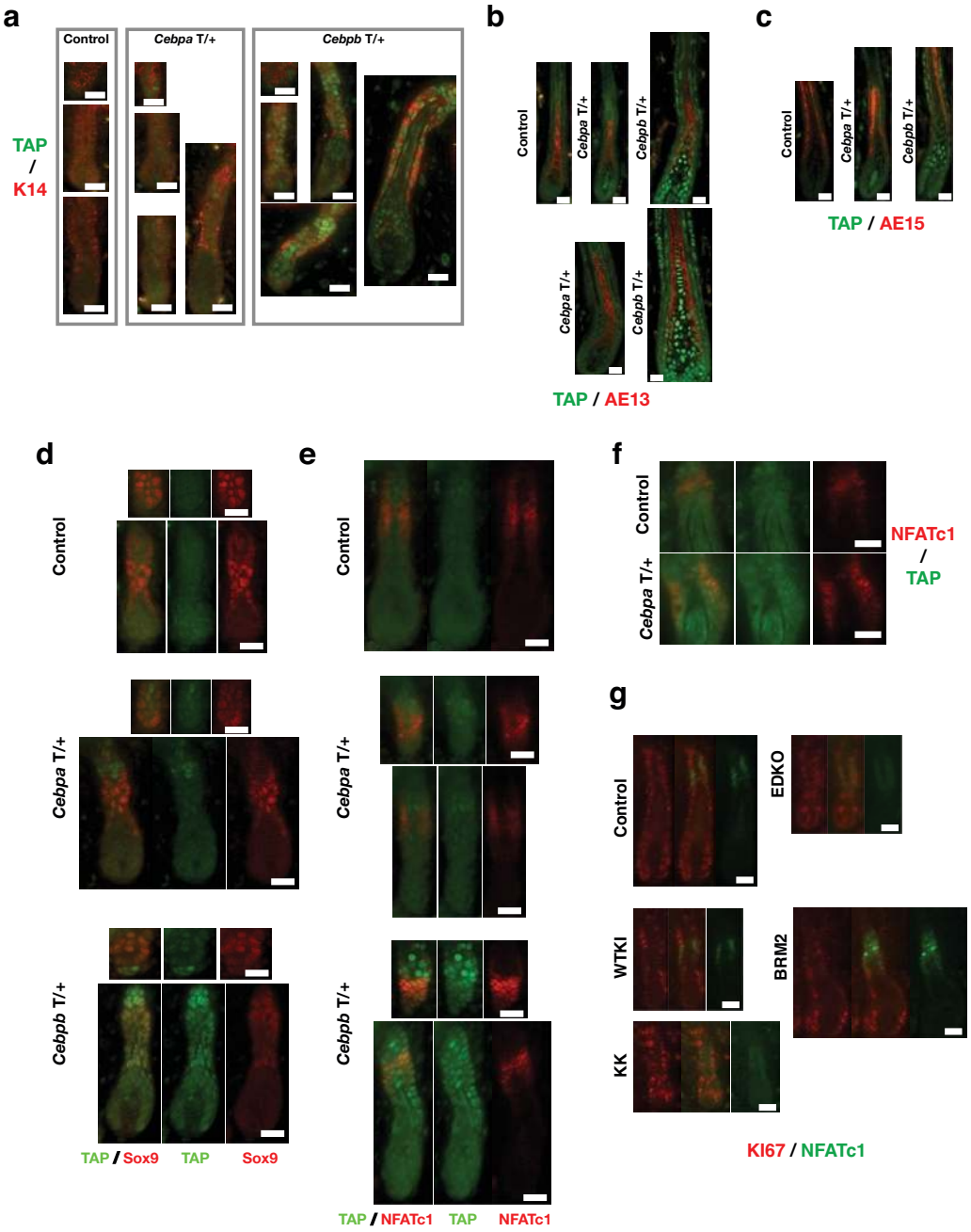

Figure S4 TAP co-stainings with HF differentiation and stem cell markers in control and C/EBP-TAP knock-in mutants - Ki67 staining in HF of controls and C/EBP mutant newborn mice. Panels a-c: Immunofluorescence microscopy was performed on skin sections of wild–type (control, left serie), Cebpa-TAP (*Cebpa*$^{T/+}$, middle serie), Cebpb-TAP (*Cebpb*$^{T/+}$, right serie) P0 (panel a) or P4 mice (panels b, c). (**a**) P0 hair follicles of different developmental stages are represented for each genotype. TAP was co-stained with K14 outer root sheat (ORS) undifferentiated keratinocyte marker. (**b**) P4 hair follicles are represented for each genotype. TAP was co-stained with AE13 hair shaft differentiation marker. (**c**) P4 hair follicles are represented for each genotype. TAP was co-stained with AE15, the trychohyalin layer of inner root sheat (IRS) differentiation marker. Panels d-f: Immunofluorescence microscopy was performed on skin sections of wild–type (control, top series); Cebpa-TAP (*Cebpa*$^{T/+}$, middle series); Cebpb-TAP (*Cebpb*$^{T/+}$, bottom series) P0 newborn mice. P0 hair follicles of two developmental stages are represented for each genotype. (**d**) TAP/Sox9 overlay, TAP and Sox9 staining (left, middle and right panel, respectively). (**e**) TAP/NFATc1 overlay, TAP and NFATc1 staining (left, middle and right panel, respectively). (**f**) Same as in (**e**) for control (top series) and Cebpa-TAP (bottom series) with a higher exposure time for TAP detection. Panel g: Immunofluorescence microscopy was performed on skin sections from *Cebpa*$^{fl/fl}$; *Cebpb*$^{fl/fl}$ (control for EDKO, left top series); *Cebpa*$^{fl/fl}$; *Cebpb*$^{fl/fl}$; K14-Cre$^{tg/+}$ (EDKO, middle top series); *Cebpa*$^{WT/fl}$; *Cebpb*$^{fl/fl}$; K14-Cre$^{tg/+}$(WTKI: control for BRM2 and KK, right top series); *Cebpa*$^{BRM2/fl}$; *Cebpb*$^{fl/fl}$; K14-Cre$^{tg/+}$ (BRM2, right bottom series) and *Cebpa*$^{KK/fl}$; *Cebpb*$^{fl/fl}$; K14-Cre$^{tg/+}$ (KK, left bottom series) P0 newborn mice. Ki67 and NFATc1 staining in hair follicles are shown for each genotype. The NFATc1 staining is used to localize the HF presumptive bulge area. In each serie corresponding to each genotype, the left panel corresponds to Ki67 staining, the middle panel to Ki67/NFATc1 overlay and the right panel to NFATc1 staining. Note that NFATc1 is nuclear in control, WTKI and BRM2 mutants, while cytoplasmic in EDKO and KK mutants. Color-coding is according to secondary antibody. Scale bars: 20 μm.

Table S1 Deregulated genes in C/EBP epidermis mutants. Differentially regulated genes for EDKO, KK, and BRM2 mutants relative to control. GCRMA-normalized probe sets passing a gap filter were fit to linear models and tested for deregulation using the LIMMA package. Probe sets that had an adjusted p-value of $P < 0.05$ for any of the mutant-vs-control tests are shown. A positive log2 fold change indicates enrichment in the mutant versus control. Blank = no significant deregulation.

Table S2 Summary of GSEA results for stem cell gene sets. Gene sets indicative of stem cells were tested for enrichment in each of the mutant genotypes (EDKO, KK, and BRM2) relative to control. Sets with a positive normalized enrichment score (NES) are enriched in the mutant and sets with a negative NES are enriched in the control. FDR q values of less than 0.25 are in red and nominal P values of less than 0.05 are in blue. Gene Set IDs correspond to the row labels in Figure 7a.

Table S3 Myc Binding sites versus C/EBP binding sites in leading edge genes. Binding site enrichment in promoters from leading edge (LedgeProm) versus random (RandomProm) genesets. Number and frequency of genes having one or more matches for the indicated TRANSFAC motifs are shown. The statistical significance of the difference (hypergeometric test) is shown. Note that neither C/EBP, nor Sox or MyoD control motifs are enriched, whereas 4/6 Myc/Max binding motifs are significantly enriched in the leading edge promoters.